US Army Corps of Engineers

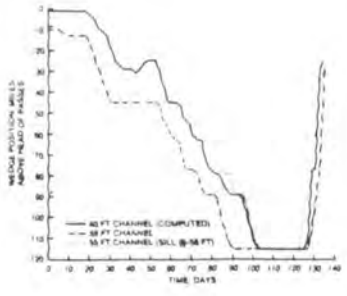

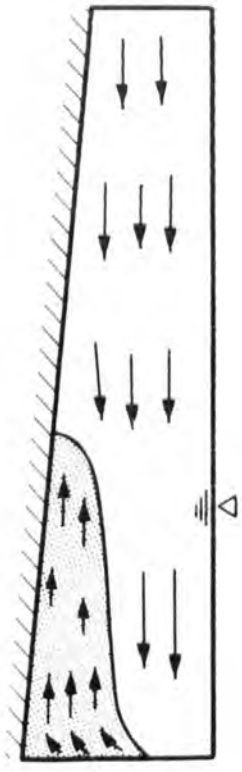

HYDRAULICS LABORATORY

TECHNICAL REPORT HL-87-1

A MATHEMATICAL STUDY OF THE IMPACT ON SALINITY INTRUSION OF DEEPENING THE LOWER MISSISSIPPI RIVER NAVIGATION CHANNEL

by

Billy H. Johnson, Marden B. Boyd, Garbis H. Keulegan

Hydraulics Laboratory

DEPARTMENT OF THE ARMY
Waterways Experiment Station, Corps of Engineers
PO Box 631, Vicksburg, Mississippi 39180-0631

April 1987
Final Report

Prepared for US Army Engineer District, New Orleans
New Orleans, Louisiana 70160

Destroy this report when no longer needed. Do not return it to the originator.

The findings in this report are not to be construed as an official Department of the Army position unless so designated by other authorized documents.

The contents of this report are not to be used for advertising, publication, or promotional purposes. Citation of trade names does not constitute an official endorsement or approval of the use of such commercial products.

REPORT DOCUMENTATION PAGE

Form Approved
OMB No. 0704-0188

1a. REPORT SECURITY CLASSIFICATION
Unclassified

1b. RESTRICTIVE MARKINGS

2a. SECURITY CLASSIFICATION AUTHORITY

2b. DECLASSIFICATION / DOWNGRADING SCHEDULE

3. DISTRIBUTION / AVAILABILITY OF REPORT
Approved for public release; distribution unlimited

4. PERFORMING ORGANIZATION REPORT NUMBER(S)
Technical Report HL-87-1

5. MONITORING ORGANIZATION REPORT NUMBER(S)

6a. NAME OF PERFORMING ORGANIZATION
USAEWES
Hydraulics Laboratory

6b. OFFICE SYMBOL (If applicable)
WESHP

7a. NAME OF MONITORING ORGANIZATION

6c. ADDRESS (City, State, and ZIP Code)
PO Box 631
Vicksburg, MS 39180-0631

7b. ADDRESS (City, State, and ZIP Code)

8a. NAME OF FUNDING / SPONSORING ORGANIZATION
USAED, New Orleans

8b. OFFICE SYMBOL (If applicable)

9. PROCUREMENT INSTRUMENT IDENTIFICATION NUMBER

8c. ADDRESS (City, State, and ZIP Code)
PO Box 60267
New Orleans, LA 70160-0267

10. SOURCE OF FUNDING NUMBERS

PROGRAM ELEMENT NO.	PROJECT NO.	TASK NO.	WORK UNIT ACCESSION NO.

11. TITLE (Include Security Classification)
A Mathematical Study of the Impact on Salinity Intrusion of Deepening the Lower Mississippi River Navigation Channel

12. PERSONAL AUTHOR(S)
Johnson, Billy H., Boyd, Marden B., Keulegan, Garbis H.

13a. TYPE OF REPORT	13b. TIME COVERED	14. DATE OF REPORT (Year, Month, Day)	15. PAGE COUNT
Final report	FROM _____ TO _____	April 1987	76

16. SUPPLEMENTARY NOTATION
Available from National Technical Information Service, 5285 Port Royal Road, Springfield, VA 22161.

17. COSATI CODES		
FIELD	GROUP	SUB-GROUP

18. SUBJECT TERMS (Continue on reverse if necessary and identify by block number)
Lower Mississippi River
Mathematical models
Navigation
Salinity
Sills (Geology)

19. ABSTRACT (Continue on reverse if necessary and identify by block number)

One factor being considered in the evaluation of the feasibility of deeper draft access to the ports of New Orleans and Baton Rouge is the impact of a deeper channel on salinity intrusion in the Lower Mississippi River. To address this question, a laterally averaged mathematical model called LAEM that couples the flow and salinity computations through a baroclinic contribution to the longitudinal pressure gradient has been employed for 40-, 45-, 50- and 55-ft channels (with overdepth dredging) using historical low-flow hydrographs. In addition, LAEM has been applied with increased heights of the natural river crossing at river mile 63.4 to determine if such sills provide an effective means of controlling salinity intrusion during critically low-flow periods. A separate question concerning the stability of such sills constructed from natural river sediment dredged from upstream has been addressed by applying the sediment transport model, HEC-6.

(Continued)

20. DISTRIBUTION / AVAILABILITY OF ABSTRACT
☒ UNCLASSIFIED/UNLIMITED ☐ SAME AS RPT ☐ DTIC USERS

21. ABSTRACT SECURITY CLASSIFICATION
Unclassified

22a. NAME OF RESPONSIBLE INDIVIDUAL

22b. TELEPHONE (Include Area Code)

22c. OFFICE SYMBOL

DD Form 1473, JUN 86 *Previous editions are obsolete.*

19. ABSTRACT (Continued).

General conclusions are that an increased channel depth up to 55 ft will result in significant increases in the extent and duration of salinity intrusion during extended low-flow periods. Sills constructed at a crossing by depositing material dredged from upstream appear to provide an effective method for controlling the intrusion of the salt wedge, although tests on a sill at elevation -55 ft indicated the deposited material will be eroded away fairly quickly when the riverflow rises above 400,000 cfs. This will necessitate rebuilding the sill at the onset of each critically low-flow period expected on the Lower Mississippi River.

PREFACE

The work described herein and the preparation of this report were conducted during portions of 1981-1986 for the US Army Engineer District, New Orleans, by the US Army Engineer Waterways Experiment Station (WES) under the general supervision of Messrs. H. B. Simmons and F. A. Herrmann, Jr., Chiefs of the Hydraulics Laboratory, and M. B. Boyd, Chief of the Hydraulic Analysis Division (HAD).

Drs. B. H. Johnson, G. H. Keulegan, and Mr. Boyd conducted the study and prepared this report. Mr. R. R. Copeland, HAD, assisted by conducting the sill stability tests. This report was edited by Mrs. Beth Burris with Mrs. Chris Habeeb coordinating the final layout.

COL Allen F. Grum, USA, was the previous Director of WES. COL Dwayne G. Lee, CE, is the present Commander and Director. Dr. Robert W. Whalin is Technical Director.

CONTENTS

CONVERSION FACTORS, NON-SI TO SI (METRIC) UNITS OF MEASUREMENT

Non-SI units of measurement used in this report can be converted to SI (metric) units as follows:

Multiply	By	To Obtain
cubic feet per second	0.02831685	cubic metres per second
feet	0.3048	metres
feet per second	0.3028	metres per second
miles (US statute)	1.609344	kilometres
tons (2,000 lb, mass)	907.1847	kilograms

A MATHEMATICAL STUDY OF THE IMPACT ON SALINITY INTRUSION OF DEEPENING THE LOWER MISSISSIPPI RIVER NAVIGATION CHANNEL

PART I: INTRODUCTION

Background

1. The US Army Engineer District, New Orleans (LMN), has been evaluating the feasibility of deeper draft access to the ports of New Orleans and Baton Rouge, Louisiana. One of the factors being considered in the evaluation is the impact of the deeper channel on salinity intrusion in the Lower Mississippi River. The importance of such an evaluation is because the city of New Orleans relies primarily upon the Mississippi River for its supply of fresh water.

Approach

2. An analysis of this factor was accomplished several years ago by the LMN and employed basically a steady-flow approach that assumed a channel of constant width and depth. The Hydraulics Laboratory, US Army Engineer Waterways Experiment Station (WES), was asked if other approaches were available that could provide additional insight into the extent and duration of salinity intrusion with different low-flow hydrographs and channel sizes. Hydraulic Analysis Division personnel suggested a dynamic analysis of the salinity intrusion phenomena using actual channel cross sections. This approach involved adapting an existing two-dimensional breadth-averaged hydrodynamic model to the Lower Mississippi River. The model (Laterally Averaged Estuarine Model (LAEM)) was developed by Edinger and Buchak (1981) and is the estuarine adaptation of a Laterally Averaged Reservoir Model (LARM) developed for CE use through contract work by Edinger and Buchak (1983) and in-house work at WES.

3. Results from an initial feasibility level analysis of the problem were presented by Boyd and Johnson (1982) to LMN in a letter report. In that report it was recommended that as the project moved into the General Design Memorandum phase, the analysis be repeated to develop predictions which reflected the latest river geometry and a more refined model verification.

4. To provide new river geometry data at key river crossings, LMN

personnel conducted hydrographic surveys in October 1982. During the analysis of these data, it was discovered that several major river crossings below New Orleans had not been accurately represented in the preliminary analysis. Since such crossings can play a major role in retarding the intrusion of the salt wedge, this reemphasized the need to reanalyze the impact of a deeper channel on salinity intrusion using recent geometry data at the crossings. Also, in the initial analysis, only a very limited study of the sensitivity of model results to diffusion coefficients and downstream boundary conditions on salinity and the water-surface elevation was attempted. In the study reported herein, a more detailed analysis of these factors is presented.

Purpose

5. A major reason for conducting the numerical modeling study was not only to evaluate the impact of a deeper channel on salinity intrusion using historical riverflows but also to use the numerical model to determine the impact on the wedge intrusion of increasing the height of natural river crossings, i.e., creating a sill in the river. To address the question of the stability of such a sill composed of natural sediment, the HEC-6 computer program "Scour and Deposition in Rivers and Reservoirs," HEC (1977), was applied.

PART II: DESCRIPTION OF NUMERICAL FLOW - SALINITY MODEL

6. Under the Environmental and Water Quality Operation Study (EWQOS) program of the US Army Corps of Engineers, developmental work has been conducted for several years on a two-dimensional (2D) laterally averaged, free surface, variable density, and heat conducting model for use in simulating flows in thermally stratified reservoirs. This effort, which extended the earlier work funded by the US Army Engineer Division, Ohio River (Edinger and Buchak 1979), has resulted in a numerically efficient model that is known as LARM. Under a contract with the US Army Engineer District, Savannah, LARM has been modified for use in computing stratified flows in estuaries as a result of both salinity and thermal effects. This model is known as LAEM, Edinger and Buchak (1981), and was the model applied in the present study.

Governing Equations

7. The basic set of equations that are solved in LAEM are statements of the conservation of mass and momentum of the flow field plus the conservation of the heat and salt content of the water body. The governing equations are developed by first performing a temporal averaging of the three-dimensional equations for laminar flow. Boussinesq's eddy coefficient concept is then employed to account for the effect of turbulence in the flow field. Next, the time-averaged equations are averaged over the estuary width and finally over an individual vertical layer with boundaries at $z = k + 1/2$ and $z = k - 1/2$ to yield the following equations that are solved in LAEM:

longitudinal (x-direction momentum)

$$\frac{\partial}{\partial t}(UBh) + \frac{\partial}{\partial x}(U^2Bh) + (u_b w_b b)_{k+1/2} - (u_b w_b b)_{k-1/2}$$

$$+ \frac{1}{\rho}\frac{\partial}{\partial x}(PBh) - A_x \frac{\partial^2}{\partial x^2}(UBh) + (\tau_z b)_{k+1/2} - (\tau_z b)_{k-1/2} = 0 \qquad (1)$$

with

$$\tau_z = C^* \rho_a / \rho W_a^2 \cos \phi \quad \text{(surface)}$$

$$= A_z \, \partial U / \partial z \quad \text{(interlayer)}$$

$$= gU|U|/c^2 \quad \text{(bottom)}$$

internal continuity

$$(w_b b)_{k-1/2} = (w_b b)_{k+1/2} + \frac{\partial}{\partial x}(UBh) - qBh \tag{2}$$

total depth continuity

$$\frac{\partial(\xi b)}{\partial t} - \sum_k \frac{\partial}{\partial x}(UBh) = \sum_k qBh \tag{3}$$

vertical (z-direction) momentum

$$\frac{\partial P}{\partial z} = \rho g \tag{4}$$

heat balance

$$\frac{\partial}{\partial t}(BhT) + \frac{\partial}{\partial x}(UBhT) + (w_b bT)_{k+1/2} - (w_b bT)_{k-1/2}$$

$$- \frac{\partial}{\partial x}\left(D_x \frac{\partial BhT}{\partial x}\right) - \left(D_z \frac{\partial BT}{\partial z}\right)_{k+1/2} + \left(D_z \frac{\partial BT}{\partial z}\right)_{k-1/2} = \frac{H_n Bh}{V} \tag{5}$$

salinity balance

$$\frac{\partial}{\partial t}(BhS) + \frac{\partial}{\partial x}(UBhS) + (w_b bS)_{k+1/2} - (w_b bS)_{k-1/2}$$

$$- \frac{\partial}{\partial x}\left(D_x \frac{\partial BhS}{\partial x}\right) - \left(D_z \frac{\partial BS}{\partial z}\right)_{k+1/2} + \left(D_z \frac{\partial BS}{\partial z}\right)_{k-1/2} = SqBh \tag{6}$$

equation of state

$$\rho = \left[1000\ P_o/(LA + 0.698\ P_o)\right] \tag{7}$$

where

$$P_o = 5890 + 38T - 0.375T^2 + 3S$$

$$LA = 1779.5 + 11.25T - 0.0745T^2 - (3.8 + 0.01T)S \tag{8}$$

Variables in the equations above are defined below:

A_x x-direction momentum dispersion coefficient, m^2/s

A_z z-direction momentum dispersion coefficient, m^2/s

b Estuary or river width, m

B Laterally averaged width integrated over h , m

c Chezy resistance coefficient, $m^{1/2}/s$

C* Resistance coefficient associated with wind

D_x x-direction temperature and salinity dispersion coefficient, m^2/s

D_z z-direction temperature and salinity dispersion coefficient, m^2/s

g Acceleration due to gravity, m/s^2

h Horizontal layer thickness, m

H_n Source strength for heat balance, $^oC\ m^3\ s^{-1}$

k Integer layer number, positive downward

P Pressure, N/m^2

q Tributary inflow or withdrawal, m^3/s

S Laterally averaged salinity integrated over h , ppt

t Time (s)

T Laterally averaged temperature integrated over h , ^oC

u_b x-direction, laterally averaged velocity, m/s

U x-direction, laterally averaged velocity integrated over h , m/s

V Cell volume ($B \cdot h \cdot \Delta x$), m^3

W_a Wind speed, m/s

w_b z-direction, laterally averaged velocity, m/s

x and z Cartesian coordinates: x is along the estuary center line at the water surface, positive to the right and z is positive downward from the x-axis, m

Δx Longitudinal spatial step, m

Δt Timestep, sec

ξ Surface elevation, m

ρ Density, kg/m^3

ρ_a Air density, kg/m^3

τ_z Tangential stress in positive x-direction divided by the water density, m^2/s^2

ϕ Wind direction, rad

8. Basic assumptions in addition to the reduced dimensionality are that the Boussinesq approximation (ρ is constant except where multiplied by the acceleration of gravity) is applicable and that vertical accelerations are negligible so that the pressure can be considered hydrostatic. In addition, the concept of eddy coefficients is utilized to represent the effect of both time averaging, as previously noted, and spatial averaging of the equations. The horizontal dispersion coefficients, A_x and D_x, are assumed to be constant, whereas the vertical dispersion coefficients, A_z and D_z, are dependent upon the stratification as reflected by the local Richardson number, (R_i) i.e.

$$A_z = A_{z_o} (1 + 3.33R)^{-3/2}$$

$$D_z = D_{z_o} (1 + 10R_i)^{-1/2} \tag{9}$$

where

$$R_i = \frac{\frac{g}{\rho}\left(\frac{\partial \rho}{\partial z}\right)}{\left(\frac{\partial U}{\partial z}\right)^2} \tag{10}$$

and A_{z_o} and D_{z_o} are the vertical coefficients for no stratification. Due to the hydrostatic pressure assumption, unstable stratification cannot be modeled in a convective fashion and thus is handled in a diffusive manner by increasing D_z to its stability limit of $h^2/2\Delta t$, where Δt is the computation time-step.

9. The laterally averaged horizontal pressure gradient in the longitudinal momentum equation contains the density driving force. Using the expression for the hydrostatic pressure, the horizontal pressure gradient can be divided into its two components of the barotropic (surface slope) gradient and the baroclinic (density) gradient to yield:

$$\frac{\partial p}{\partial x} = -g\rho \frac{\partial \xi}{\partial x} + g \int_{\xi}^{z} \left(\frac{\partial \rho}{\partial x}\right) dz \tag{11}$$

Numerical Solution Scheme

10. Finite difference techniques are employed to solve the governing Equations 1-7. The particular scheme employed is structured such that the water-surface elevations are computed implicitly. Using the new water-surface elevations, the x-component of the flow velocity is then explicitly computed from the longitudinal momentum equation. As in other hydrostatic models, the vertical component of the velocity is computed from the continuity equation which is reduced to the incompressibility condition as a result of the Boussinesq approximation. The solution begins at the bottom and progresses up the column of layers. With the flow field computed, the water temperature and salt concentration are then computed from their respective transport equations in an implicit fashion. A detailed discussion of the solution scheme can be found in the report by Edinger and Buchak (1979).

11. The major advantage of the solution scheme employed in LAEM is that the extremely restrictive stability criterion based upon the speed of the free surface gravity wave, i.e. $\Delta t < (\Delta x/\sqrt{gH_{max}})$, where H_{max} is the maximum water depth, is removed. However, since the convective terms and density gradient in the longitudinal momentum equation, as well as the vertical diffusion term in the temperature and salt transport equations, are lagged in an explicit fashion the following stability criteria still remain:

$$\Delta t < \frac{\Delta x}{U}$$

$$\Delta t < \frac{\Delta x}{\sqrt{\frac{\Delta\rho}{\rho} g h_w}} \qquad (12)$$

and

$$\Delta t < \frac{h^2}{2D_z}$$

where h is the layer thickness, $\Delta\rho$ is the density difference of the fresh and saline water, and h_w is the height of the density flow.

12. The finite difference grid employed in LAEM is the marker and cell grid employed by Leendertse (1967) and others in 2-D vertically averaged models. As shown below, the velocity components are defined on the faces of a cell, with the water temperature, salinity, and corresponding density defined at the center

COMPUTATIONAL GRID

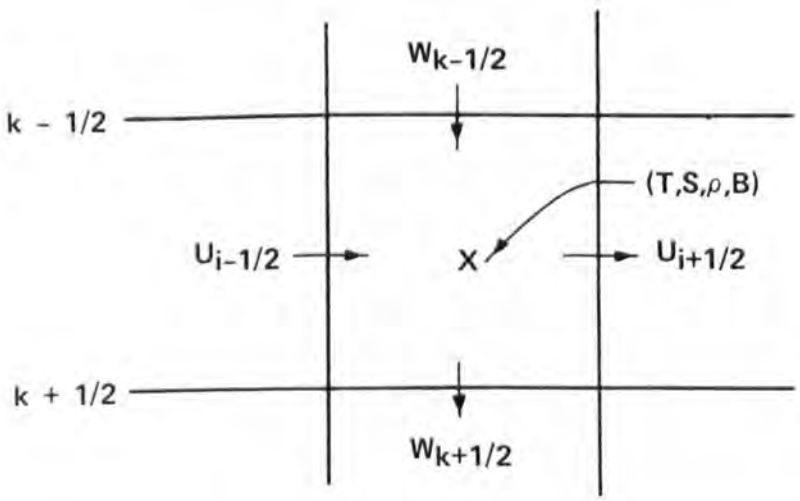

Values of variables needed at locations where they are not defined are obtained by averaging, e.g. $w_{b_{\text{cell center}}} = 1/2\ (w_{b_{k-1/2}} + w_{b_{k+1/2}})$.

Data Requirements

13. The major data input required by LAEM is the geometry data describing the system. At the center of each computational cell the width of

the estuary or river must be prescribed. For the study described herein, these were obtained from hydrographic survey data furnished by the Lower Mississippi Valley Division (LMVD) and LMN. Additional data required are the boundary conditions that drive the internal flow field. At the river boundary, a discharge hydrograph must be prescribed, whereas at the ocean boundary the tide must be input. In addition, at inflow boundaries the temperature and salinity must be prescribed. In the present study, the water temperature was assumed constant and the surface heat exchange was set to zero. However, for problems in which thermal effects are considered, shortwave solar radiation, air temperature, dew-point temperature, and wind speed must be known in order to compute the coefficients required in the computation of the rate of surface heat exchange.

PART III: SYSTEM DESCRIPTION AND SCHEMATIZATION

System Schematization

14. Figure 1 is a map showing the Mississippi River from Baton Rouge at mile 228.4 AHP* to the Gulf of Mexico. This segment of the Mississippi River, which would be deepened and/or widened where necessary to provide a 750-ft-wide** by 45-, 50- or 55-ft-deep navigation channel (with overdepth dredging), was schematized in the modeling effort (Figure 2). At the Gulf where flow exits through three major distributaries (Southwest Pass, South Pass, and Pass a Loutre) and several smaller ones, it was assumed that the system could be satisfactorily reproduced by treating Southwest Pass as the dominant distributary and representing outflow through the other distributaries as lateral outflows at the appropriate locations. This assumption also implies that wedge intrusion into the system is dominated by saline water moving up Southwest Pass. These assumptions were discussed with WES and LMN personnel, who have extensive experience with the passes area, and appear reasonable for the existing situation. They will be even more appropriate under future conditions as South Pass continues to shoal from the earlier maintained navigation depth of 30 ft to a controlling depth of about 17 ft, similar to the controlling depth that now exists in Pass a Loutre. The dredging of a deeper navigation channel would also tend to make the assumptions more accurate.

Flow Distribution in Distributaries

15. Using the approach described above, it was necessary to prescribe the distribution of flow through the different distributaries. Discussions with WES and LMN personnel provided general guidance concerning the appropriate distribution. A one-dimensional unsteady flow model, System 11, developed by the Danish Hydraulic Institute, has been applied to the passes area.† This work, which used the most accurate geometric data available to describe

---

* AHP - Above Head of Passes.

** A table of factors for converting non-SI units of measurement to SI (metric) units is presented on page 3.

† Personal communication, R. Athow (1981), Hydraulics Laboratory, US Army Engineer Waterways Experiment Station, Vicksburg, Miss.

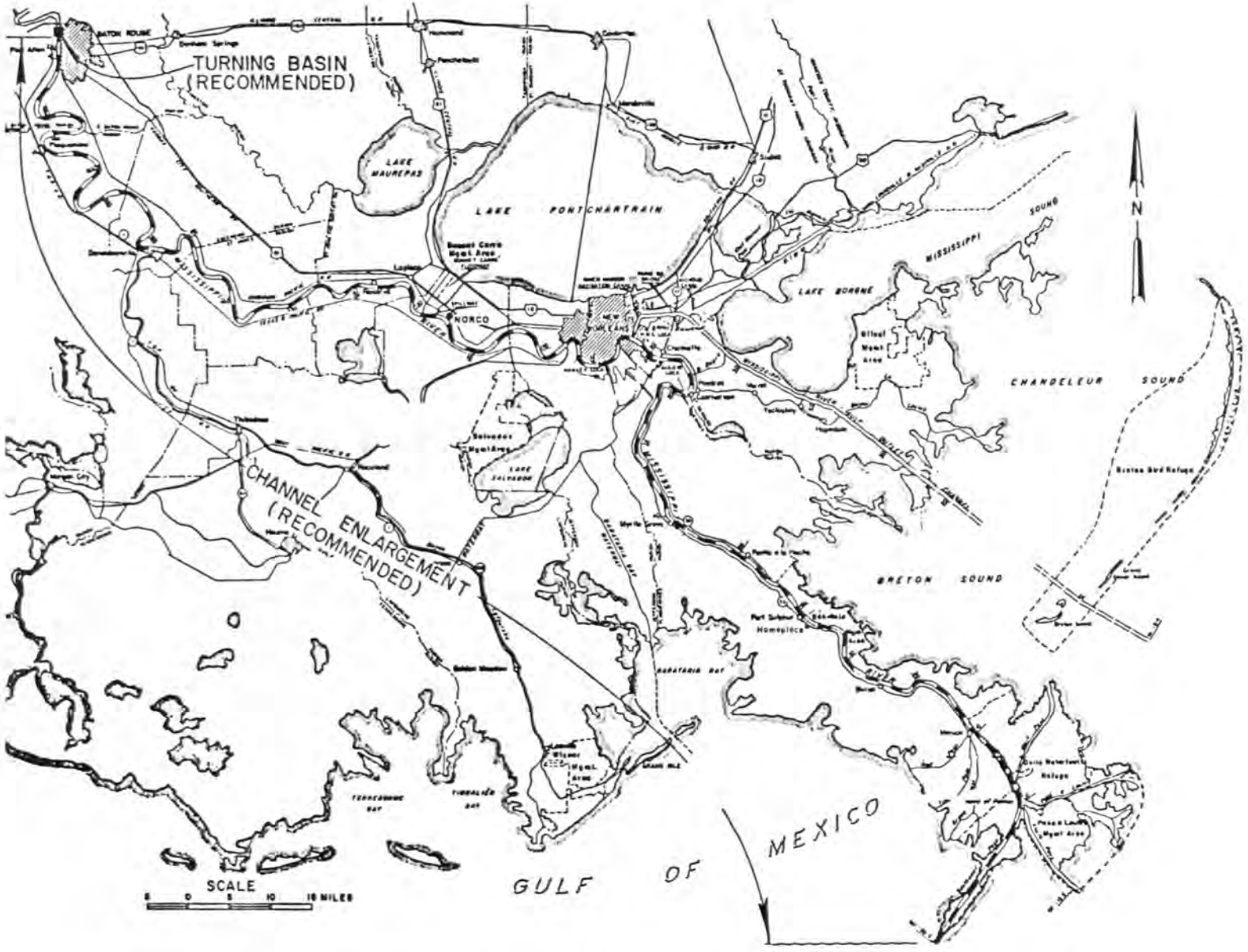

Figure 1. Location map of study reach

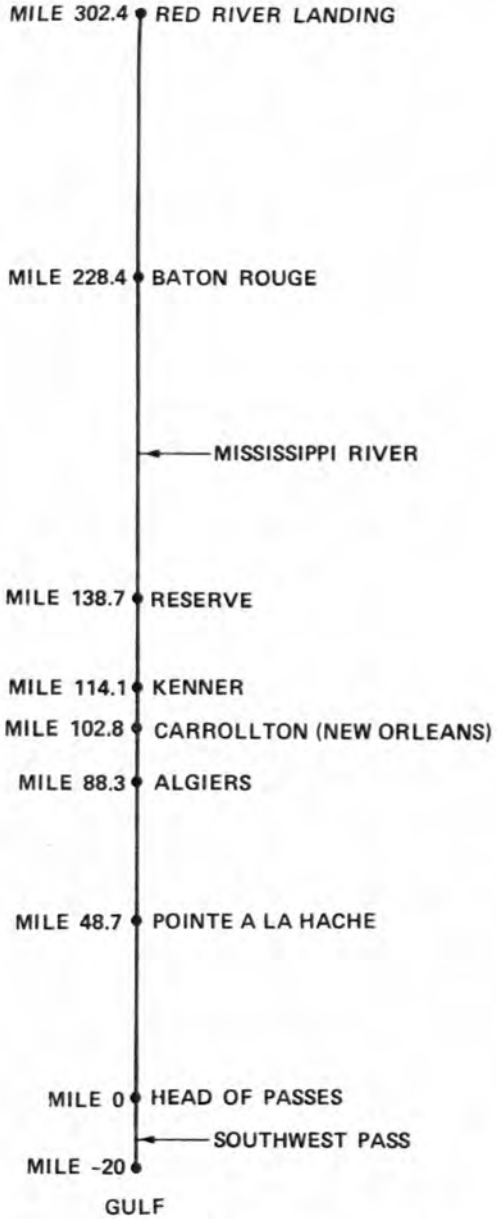

Figure 2. Schematic of Lower Mississippi River

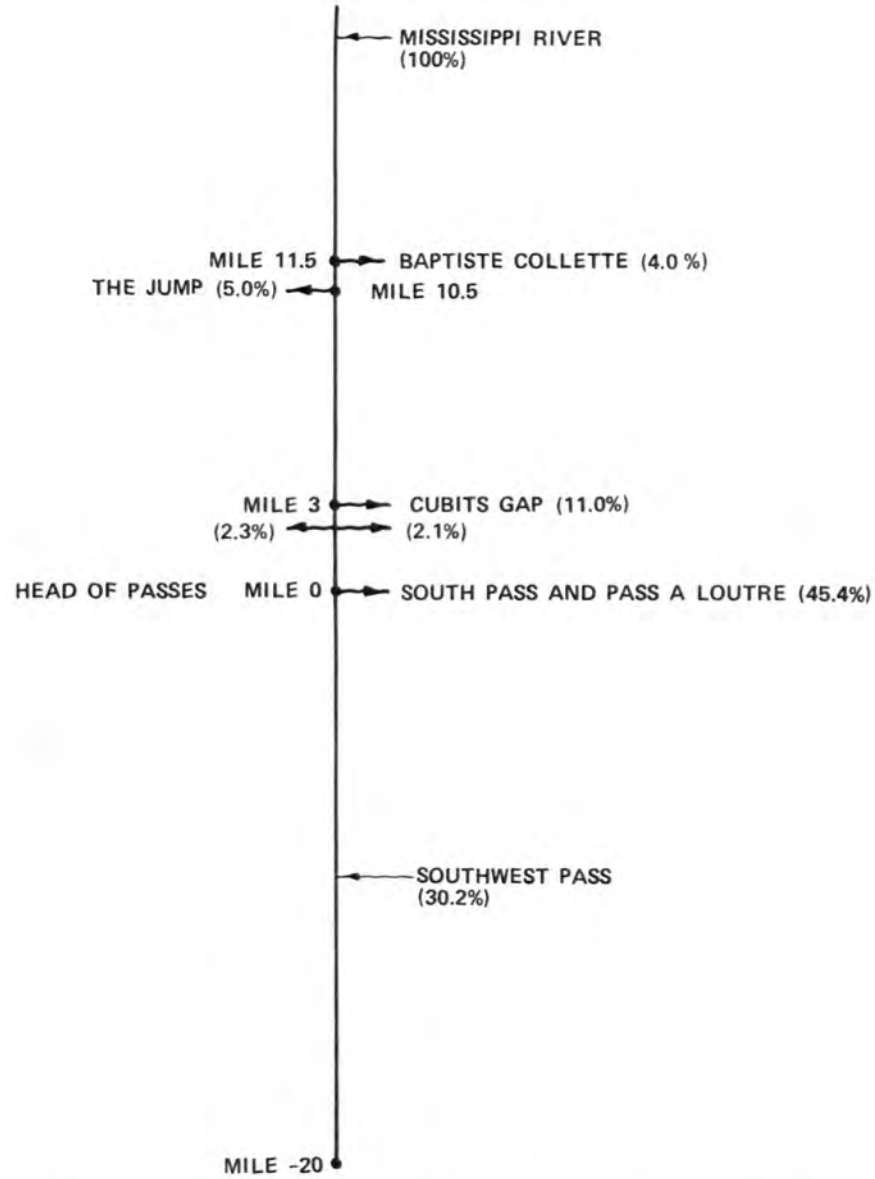

Figure 3. Mississippi River Passes approximate flow distribution

the complex distributary system, provided estimates of outflow in each distributary that were used in the 1982 study by Boyd and Johnson. However, it was decided that the flow distribution more recently provided by LMN would be used in the current work by making the assumption that the distribution provided would be reasonably appropriate for the discharge range of interest (roughly 100,000 to 300,000 cfs). The distribution specified was:

Distributary	Approximate River Mile	Percent of Flow
Baptiste Collete	11.5	4.0
The Jump	10.5	5.0
Cubits Gap	3	11.0
East Bank	3	2.1
West Bank	3	2.3
South Pass and Pass a Loutre	0	45.4

As illustrated in Figure 3, this leaves 30.2 percent of the riverflow to be discharged through Southwest Pass as opposed to 36.8 percent in the earlier study.

Channel Geometry

16. Hydrographic survey information obtained during the period 1973-1975 was used to develop channel sections for the feasibility study model. Cross-section data at intervals from about 1/2 mile to 3 miles were furnished by LMVD and/or LMN. To conserve computer time, the vertical grid used in the model ended at a depth of 100 ft. Plots of the individual cross sections were inspected, and where appropriate, adjustments were made in channel widths above -100 ft to roughly conserve volume. These adjusted cross sections were used in the GEDA computer code (HEC 1976) to develop the needed channel elevation-width tables at 1-mile intervals along the river between the Gulf and Baton Rouge.

17. Since major crossings in the river can have a significant impact on the salinity intrusion, it was considered necessary in the reanalysis to have an accurate representation of these crossings. A major question was whether or not the crossings reflected in the 1973-75 survey had experienced significant changes in the past 8 to 10 years. To answer this question, LMN conducted a detailed hydrographic survey of the five major crossings that would be likely to influence the intrusion of a salt wedge during low-flow periods. Cross-sectional plots of these crossings are presented in Figures 4-8,

Figure 4. Crossing at mile 115.9 from 1982 and 1973-75 data

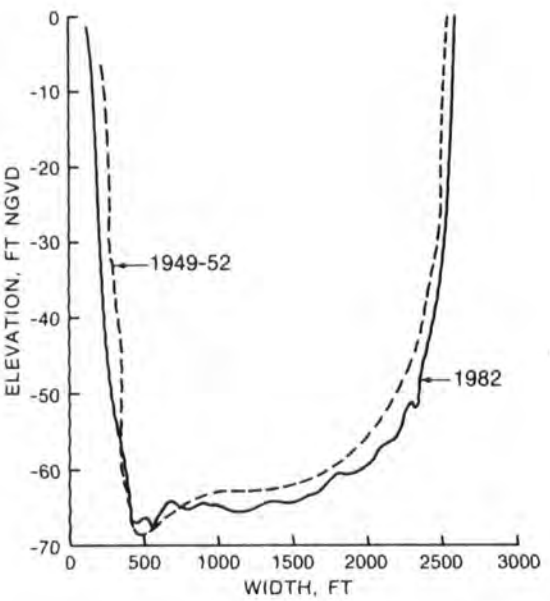

Figure 5. Crossing at mile 89.7 from 1982 data and 1949-52 data

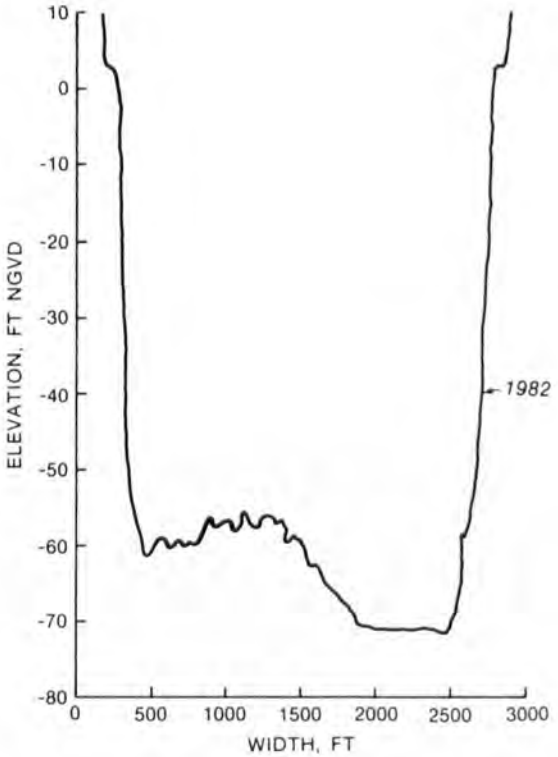

Figure 6. Crossing at mile 79.2 from 1982 data

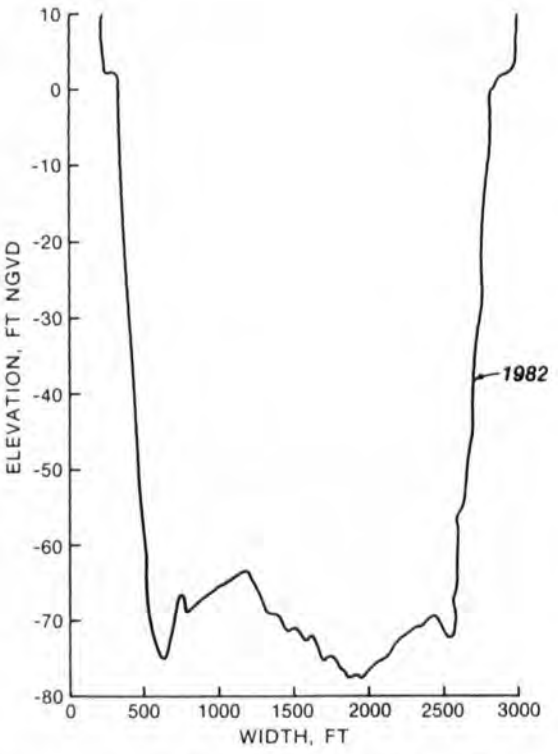

Figure 7. Crossing at mile 63.4 from 1982 data

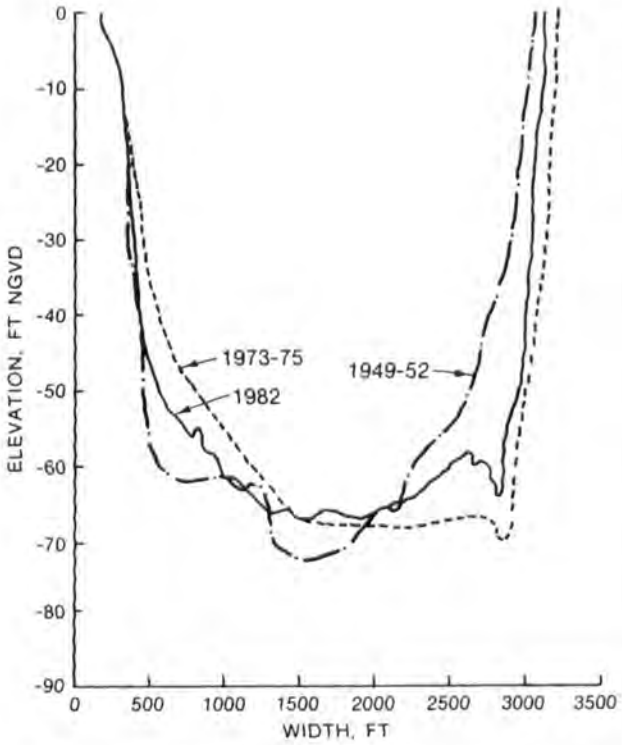

Figure 8. Crossing at mile 47.3 from 1982, 1973-75, and 1949-52 data

with Figures 4, 5, and 8 illustrating the relatively strong stability of the crossings through comparisons of 1982 sections with 1973-75 and/or 1949-52 sections.

18. Figure 9 presents a schematic of the adjusted channel bottom profile which reflects the lowest active cell in the computation grid at each point along the channel. Of course, channel widths are highly variable with elevation and along the channel. As mentioned earlier (paragraph 4), it was discovered during the analysis of the new survey data that the feasibility level study representation of some crossings did not accurately reflect the 1973-75 hydrographic data. Figure 9 shows the additional crossings that have been added to the model since the earlier study. With a longitudinal spatial step, Δx , of 2 miles and a vertical spacing of 5 ft, the computational grid is composed of (27 x 126)

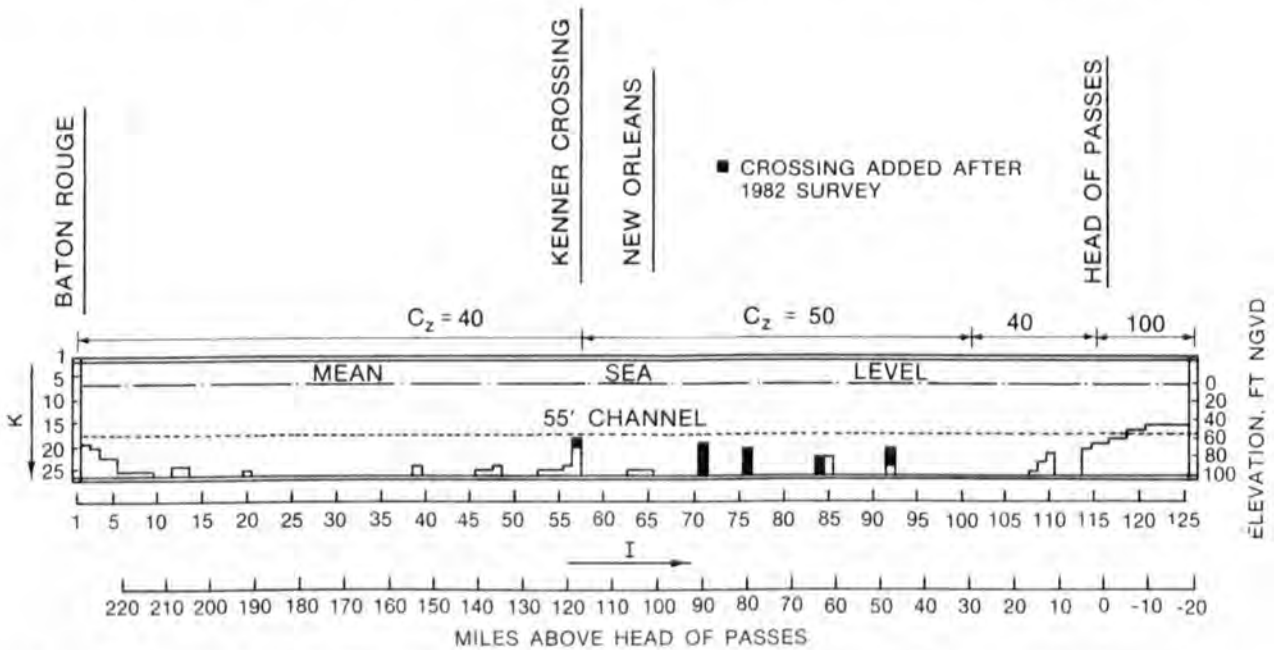

Figure 9. Schematic of channel bottom and computational grid used in LAEM

cells. In the earlier study, initial runs were made with Δx = 1 mile. However, computer experimentation revealed essentially no difference in either the flow or salinity computations when Δx was increased to 2 miles; therefore the larger value has been used in subsequent computations to save on computer costs.

19. Representation of the proposed deeper channels required deepening in Southwest Pass (indicated by the dashed line in Figure 9 for a 55-ft channel) and widening of a number of sections along the channel to provide the desired 750-width.

cells. In the earlier study, initial runs were made with Δx = 1 mile. However, computer experimentation revealed essentially no difference in either the flow or salinity computations when Δx was increased to 2 miles; therefore the larger value has been used in subsequent computations to save on computer costs.

19. Representation of the proposed deeper channels required deepening in Southwest Pass (indicated by the dashed line in Figure 9 for a 55-ft channel) and widening of a number of sections along the channel to provide the desired 750-width.

PART IV: MODEL VERIFICATION

Available Field Data

20. Since the occurrence of the 1973 flood on the Lower Mississippi River there has been no dredging of South Pass, with the channel subsequently shoaling to its current depth of about 17 ft. Recall that this resulted in the basic assumption that the salt wedge is currently primarily driven by saline waters moving through Southwest Pass which resulted in the assumption that the study reach could be modeled as a single channel extending from Baton Rouge through Southwest Pass to the Gulf. With this assumption, field data on wedge movement collected before 1973 were of limited use in verifying the model. Therefore the verification of the model was forced to rely upon a limited set of data collected during a relatively low-flow period in 1981. This set of data consists of the time-history of the tip of the wedge as well as vertical profiles of the salinity behind the tip of the wedge in January 1981. In addition, it has been generally observed that the tip of the wedge (assumed to be 9 ppt salinity or 5 ppt chloride) intrudes to the vicinity of the Head of Passes for a riverflow of about 300,000 cfs. Initially, an effort was made to ensure that the computed water-surface profiles were in reasonable agreement with field data. Stage information at Baton Rouge, New Orleans, and Venice were available for the 1980-1981 hydrograph, whereas estimates of appropriate stages for a steady riverflow of 300,000 cfs were developed using stages observed during September 1975 when the riverflow fluctuated around 300,000 cfs.

Sensitivity Runs

Influence of additional crossings

21. Figure 9 shows that the major crossing at about mile 47 was not well represented in the earlier study. Therefore the verification of the model from the earlier study, which centered around forcing the tip of the wedge to stabilize at about mile 60 for a steady riverflow of 150,000 cfs, was unlikely to be appropriate now. Figure 10 illustrates that this was indeed true since the crossing at mile 47 completely stopped the wedge for the 1980-1981 riverflows.

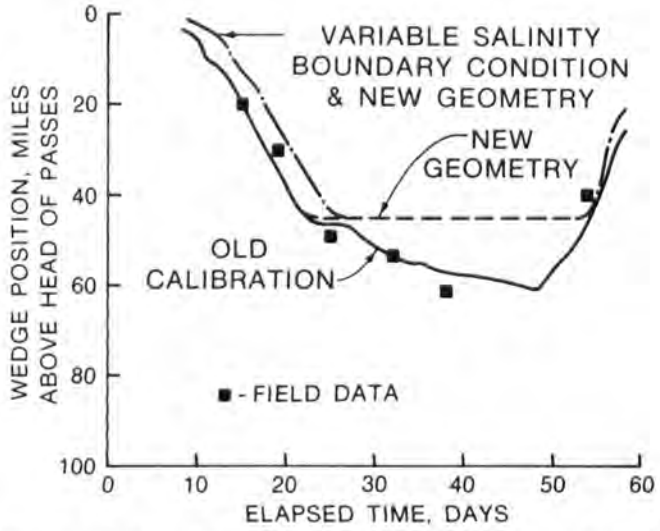

Figure 10. Effect of crossing at mile 47.3 and a variable salinity condition

Influence of salinity profiles used as boundary conditions at the Gulf

22. In the earlier study, the salinity profile used as the boundary condition at the Gulf was constructed from previous physical model tests. The profile corresponding to a riverflow of about 125,000 cfs was selected to be used over the complete range of flows encountered in the model runs (about 90,000 to 300,000 cfs). In the present study, salinity profiles corresponding to riverflows of 125,000 and 350,000 cfs were employed (Figure 11) with linear interpolation providing the boundary salinity at intermediate flows. For riverflows below 125,000 cfs, the profile corresponding to 125,000 cfs was prescribed since no additional data were known. As shown in Figure 10, the time required for the wedge to reach the crossing at mile 47 is significantly

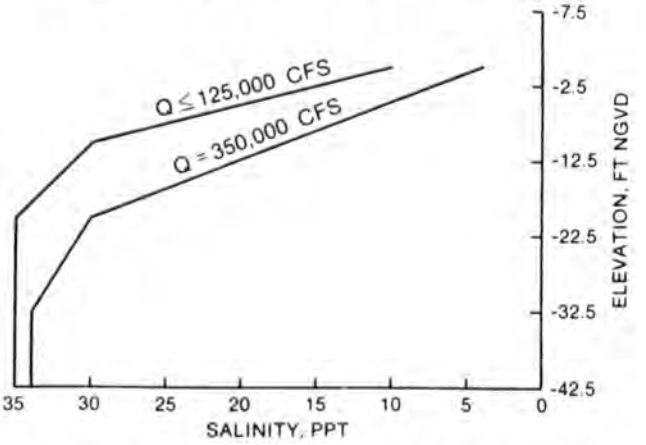

Figure 11. Variable salinity boundary condition at the Gulf

influenced when employing the variable boundary salinity condition for the 1980-1981 flows.

23. It should be noted that since the advective terms in the salinity equation are represented by one-sided differences based upon the direction of flow, only those values of the prescribed salinity profile lying in the lower cells where the denser saline water moves up the river enter into the computations. Therefore, in both a mathematical and physical sense, the downstream salinity boundary condition enters the computations properly.

Influence of vertical eddy coefficients

24. Both the x-momentum equation and the salinity transport equation contain eddy coefficients in both the x- and z-directions. Two orders of magnitude change in x-direction coefficients result in very little change in the computed flow and salinity fields. However, the model is more sensitive to variations in the vertical coefficients. As shown in Figure 12, by decreasing the vertical coefficients (D_{z_o} - salinity equation, A_{z_o} - momentum equation) by a factor of 6, the wedge can be forced to move over the crossing at mile 47 an additional 8 miles for the 1980-1981 flows. Figure 13 illustrates the influence of the vertical eddy coefficients on the salinity interface corresponding to 9 ppt. These results show that the more dominant

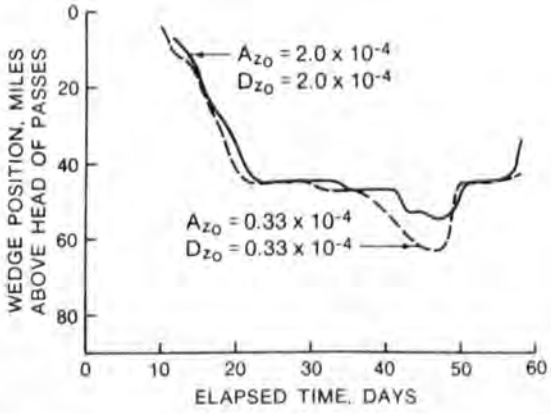

Figure 12. Effect of vertical diffusion coefficients on wedge intrusion for 1980-81 hydrograph

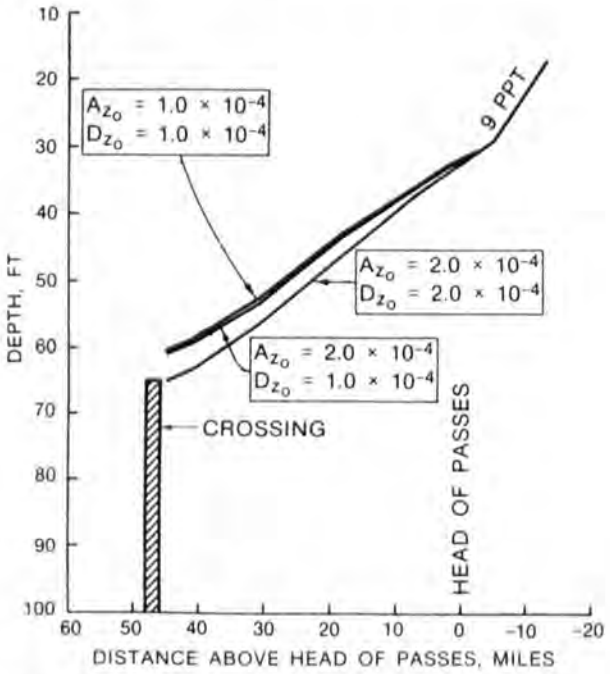

Figure 13. Effect of vertical diffusion coefficients on wedge interface for 150,000-cfs steady flow

of the two coefficients in influencing salinity intrusion is the vertical diffusion coefficient, D_{z_o}, in the salinity transport equation. Relatively large variations in A_{z_o} seem to have little influence on the computed flow field and thus little influence on the salinity field. Edinger and Buchak (1981) arrived at a similar conclusion in sensitivity studies using data from the Potomac River.

Influence of Chezy coefficient

25. The major coefficient to be varied to match a computed flow field with observed data is the Chezy coefficient, C_z. Figure 14 illustrates that the value of C_z has a major influence on the water-surface profile computed. Varying C_z from 45 $m^{1/2}$/sec to 100 $m^{1/2}$/sec results in a decrease of about 6 ft in the water surface at Baton Rouge and about 3 ft at New Orleans for a steady flow of 300,000 cfs and a Gulf elevation of 0.0 ft. Since the flow and salinity fields are coupled through the longitudinal pressure gradient, major changes in the flow field result in significant changes in the

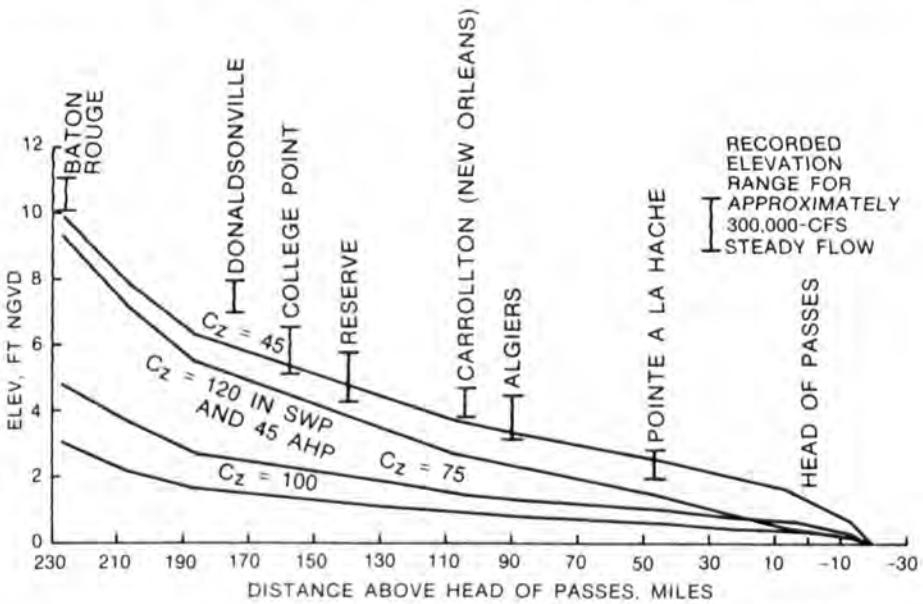

Figure 14. Effect of C_z on water-surface profile for 300,000-cfs steady flow

salinity computation. Figure 15 shows that for a steady flow of 300,000 cfs, the salt wedge only moves about 2 miles up Southwest Pass if $C_z = 45$ throughout the system, whereas the wedge stabilizes at a distance of more than 26 miles from the Gulf for $C_z = 100$.

Influence of Gulf elevation

26. The 1980-1981 hydrograph (Figure 16) was used in runs of the final

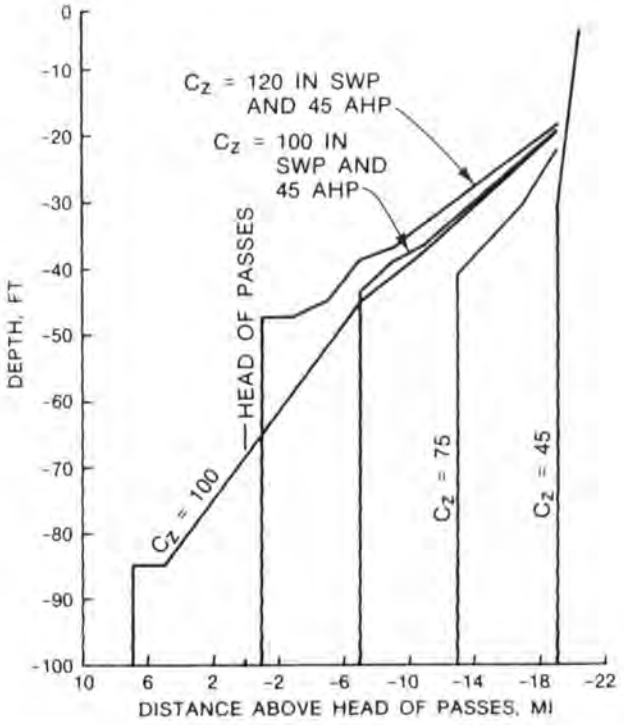

Figure 15. Effect of C_z on location of wedge interface (9 ppt) for 300,000-cfs steady flow and a variable salinity boundary condition

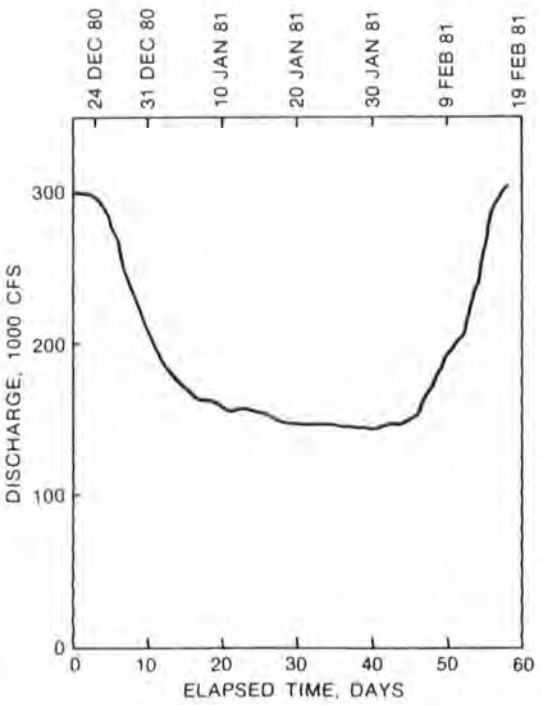

Figure 16. 1980-81 discharge used as boundary condition at Baton Rouge

verified model to investigate the influence of the Gulf elevation boundary condition on the salinity intrusion. In the earlier application of LAEM, the Gulf elevation was set to be constant at 0.0 ft NGVD after runs with a sinusoidal tide revealed no major impact on movement of the salt wedge. Therefore the initial verification of the model with the additional crossing data employed a 0.0 ft Gulf elevation also. However, after talks with WES personnel revealed that data they had analyzed seem to indicate that long term "setups" or "setdowns" occur in the Gulf, it was decided to make additional runs to determine the influence on the wedge movement of using recorded elevations in the Gulf rather than assuming a zero elevation. To accomplish this, the recorded elevations presented in Figure 17 at the Grand Isle gage were employed as the downstream boundary condition, with the discharges shown in Figure 16 as the upstream boundary condition. The location of the Grand Isle gage is some 30 to 40 miles west of the end of Southwest Pass, as illustrated in Figure 1.

27. Comparisons of computed elevations, using both a zero Gulf elevation and the Grand Isle elevations as downstream boundary conditions, versus

recorded data at Baton Rouge, New Orleans, and Venice are presented in Figures 18-20. In addition, a comparison of the water-surface profiles computed for the two cases at the end of the hydrograph when the riverflow has returned to about 300,000 cfs is presented in Figure 21. Even though the use of a zero Gulf elevation does not reflect the oscillations that are obviously occurring, in a mean sense the comparisons of recorded and computed elevations at Baton Rouge and New Orleans are in reasonable agreement while the computed elevations at Venice are about 0.5 ft too low. However, this is not the case at New Orleans and Venice when the recorded Grand Isle elevations were employed as the boundary condition at the Gulf. Making adjustments in the Chezy coefficient to force the water-surface elevations at New Orleans and Venice to match the recorded data would result in little hope of ever forcing the movement of the salt wedge to match the field data. Therefore one is faced with the question of whether or not to "believe" the Grand Isle data. The oscillations in the water surface, which may occur over several days, obviously are real. Therefore the basic problem seems to revolve around determining the proper zero of the gage, i.e., it would seem that the curve in Figure 17 should be shifted upward to yield a mean elevation of approximately zero. If it is accepted that the mean Gulf elevation should be 0.0 ft NGVD, the next question to be addressed is the influence of the relatively long-term oscillations observed in the Grand Isle data on the wedge movement. This question was answered by imposing a sinusoidal oscillation with an amplitude of 2.0 ft and a period of 10 days at the Gulf. The effect of such long-period oscillations on the wedge movement is illustrated in Figure 22. As can be seen, the long-term effect over the hydrograph is negligible and had little influence on the extent and duration of the salt intrusion. Therefore it seems reasonable to conclude that the mean water-surface level of the Gulf rather than the tidal or

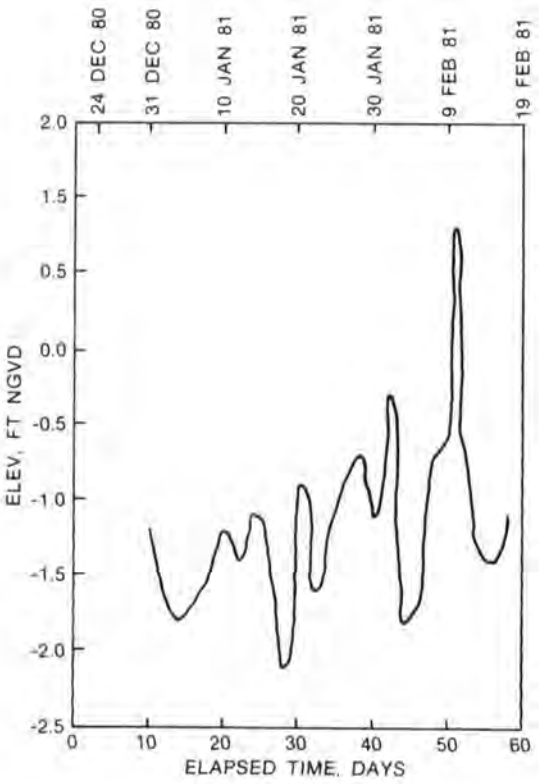

Figure 17. Recorded water-surface elevations at Grand Isle

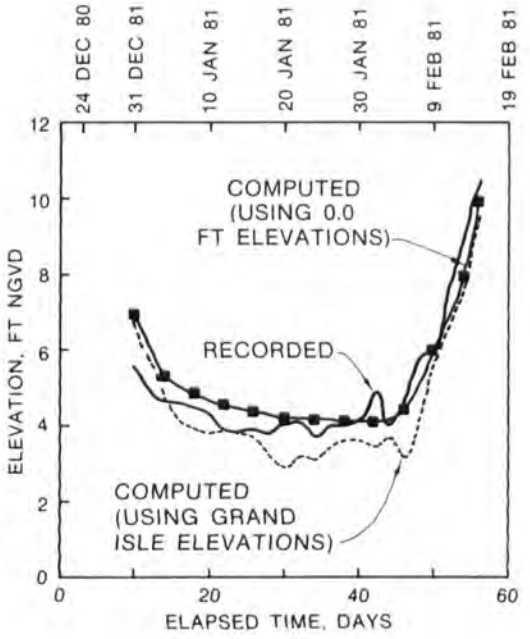

Figure 18. Comparison of computed and recorded water-surface elevations at Baton Rouge

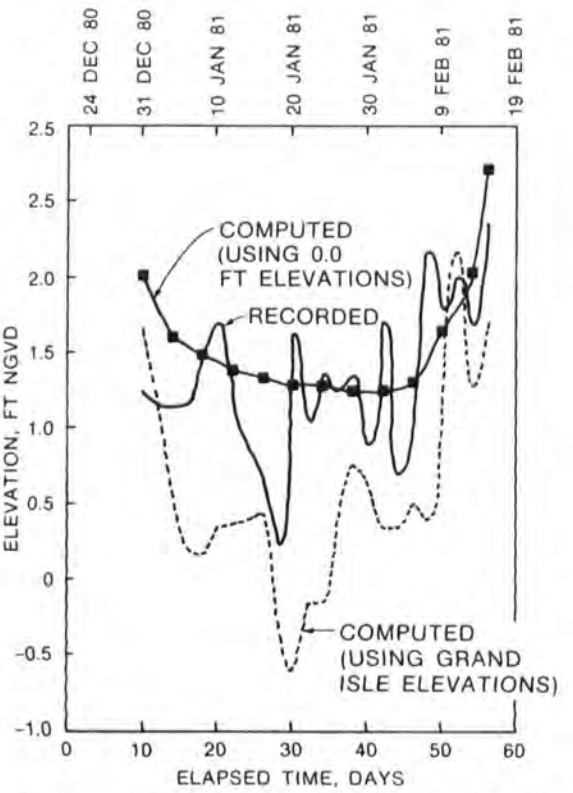

Figure 19. Comparison of computed and recorded water-surface elevations at New Orleans

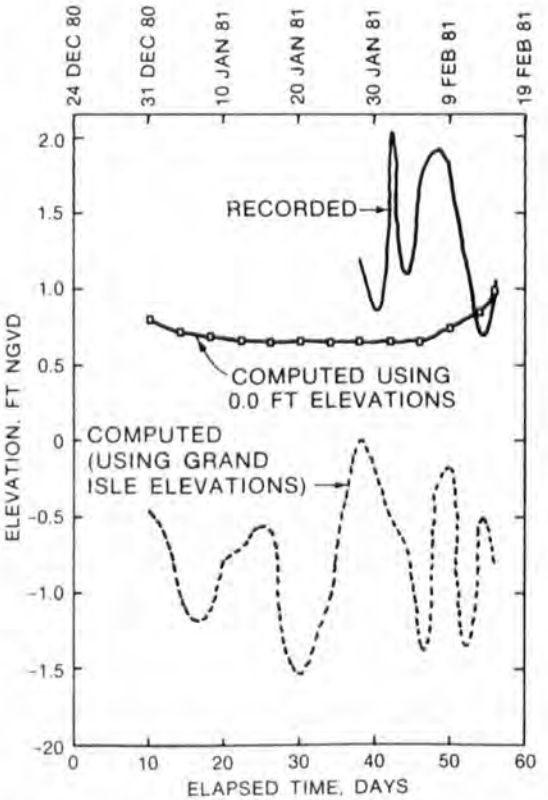

Figure 20. Comparison of computed and recorded water-surface elevations at Venice

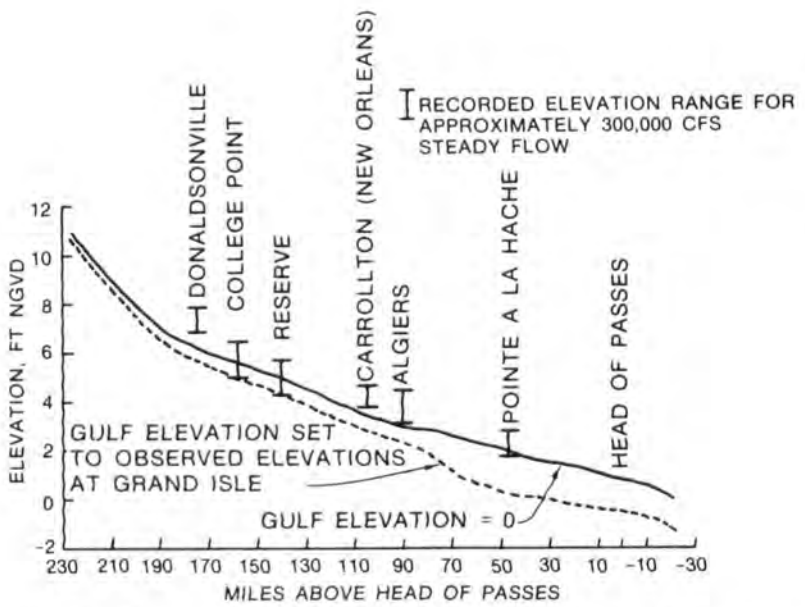

Figure 21. Effect on water-surface profile of using elevations at Grand Isle as the Gulf boundary condition

longer-period oscillations exerts the major influence on the movement of the salt wedge. Based upon these results, it seems reasonable to conclude that the use of a zero Gulf elevation as the downstream boundary condition is the appropriate condition to use in both the verification run and the series of historical hydrographs to be discussed later.

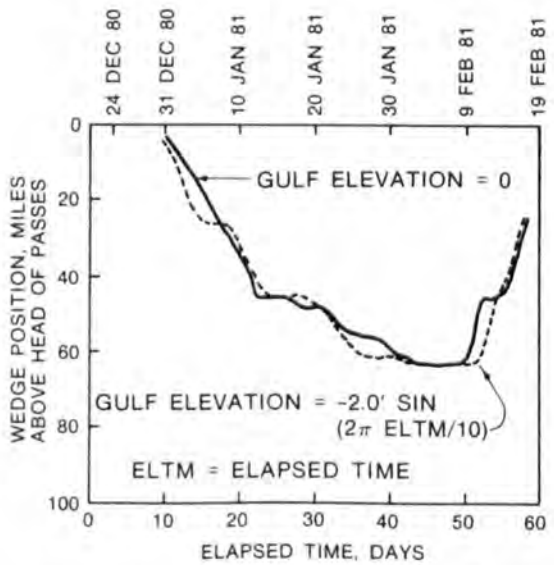

Figure 22. Effect on salinity intrusion of long period oscillations in the Gulf

Verification Results

28. As illustrated in Figure 10, after placing the additional crossings in the system, the model as calibrated from the earlier study could not reproduce the 1980-1981 field data on the wedge movement. In the earlier study, the final Chezy adjustment used a value of 100 in Southwest Pass and a value of 45 above Head of Passes. With the new crossing at mile 47, a problem in the verification exercise developed. Field data indicate that the wedge moves past the crossing and essentially stabilizes at about mile 61. Therefore adjustments in the Chezy coefficient and/or the vertical diffusion coefficient, D_{z_o}, are required to force the wedge to overtop the crossing at mile 47 fairly quickly; but the adjustments must be such that once the crossing is overtopped the wedge stops within the next 10 to 15 miles.

29. Many different combinations of the roughness and diffusion coefficients were tried. The final values of A_{z_o} and D_{z_o} selected were 1.5×10^{-4} m^2/sec and 0.5×10^{-4} m^2/sec, respectively. The model default value for both is 2.0×10^{-4} m^2/sec, which is representative of values in the Potomac River.

30. With the spatial variation of C_z shown in Figure 9, the values of A_{z_o} and D_{z_o} noted above, the variable salinity boundary condition given in Figure 11, and a zero Gulf elevation as the downstream elevation boundary condition, the final verification results on wedge movement for the 1980-1981 hydrograph are presented in Figure 23. A physical explanation for the large difference between Chezy values above and below Head of Passes is not apparent.

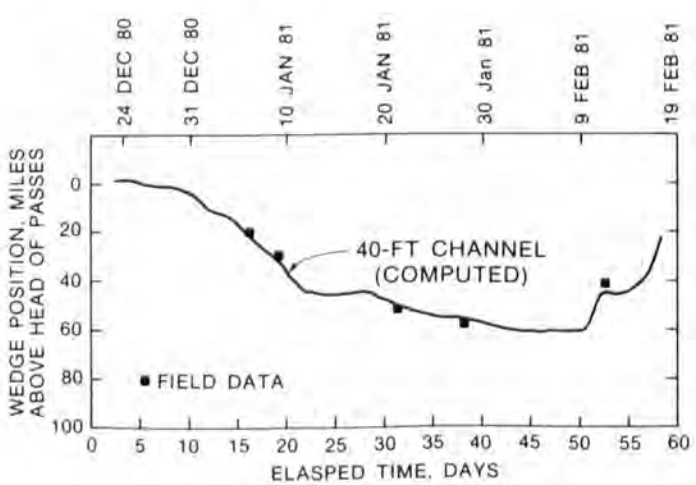

Figure 23. Model calibration of wedge position

It could indicate that the assumed flow diversions in the Passes area are not entirely correct. It might also be noted that a simplified form of the x-momentum equation is solved at the downstream boundary, which, as noted by Edinger and Buchak (1981), may result in the need for a nonphysical value of the Chezy coefficient near the downstream boundary. Using the expression $n = h^{1/6}/C_z$ to convert the Chezy coefficient to the more commonly employed Manning roughness coefficient in river studies yields corresponding n-values of 0.015 in Southwest Pass and about 0.035 in the river.

31. Figures 18-21 (as discussed earlier) show the comparison of computed and recorded elevations at Baton Rouge, New Orleans, and Venice plus the water-surface profile for a riverflow of approximately 300,000 cfs at the end of the 1980-1981 hydrograph. Remember that the Gulf elevation is 0.0 ft.

32. Computed and observed vertical salinity profiles are plotted in Figure 24. The field data plotted are from measurements on 28 January 1981 at a location 5 miles behind the tip of the wedge, which is located at about mile 59. The computed profile presented is on the same day, i.e., 28 January 1981, but at a distance of 8 miles behind the wedge tip. As can be seen, these results compare reasonably well with the field data. As a result of numerical diffusion in the model (exists in some degree in virtually all numerical models), the computed interface is not as sharp as the field data imply. However, the computed and recorded concentration of approximately 1.0 ppt that occurs at a depth of about 50 ft below the water surface compares well. Additional discussion on the vertical structure of the wedge is provided in PART V.

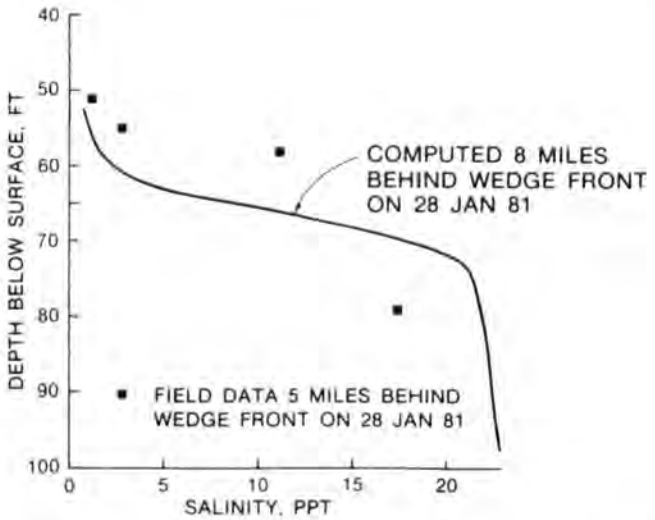

Figure 24. Vertical structure of salt wedge

33. The model as adjusted responded properly to boundary condition changes, and in general, the agreement between computed results and 1980-1981 field observations used in the verification was quite good. A set of field data for a much greater intrusion of the wedge would have been preferable; however, as previously noted, these were not available for the system as it exists today.

PART V: ARRESTED WEDGE ANALYSIS

34. Results from computations made with a constant riverflow of 150,000 cfs are used to analyze the characteristics of the arrested saline wedge formed. These are then compared with experimental results obtained by Keulegan (1949) in laboratory studies. The vertical distribution of salinity and the longitudinal component of the velocity, as well as the position of the arrested wedge interface and the interfacial shear stress, are considered.

Distribution of Salinities

35. For a steady flow of 150,000 cfs, the toe of the arrested saline wedge stabilizes at mile 61 above the Head of Passes. The computed vertical distributions of salinity at miles 8, 34, and 54 are presented in Figure 25. The common procedure is to plot the salinity as a ratio of the salinity at a particular depth and the bottom salinity, S_o. The interface surface is then taken where S/S_o equals 0.5. The freshwater depth, h_1, is the distance from the surface to that point. Figure 25 shows that the freshwater depths at miles 8, 34, and 54 are 38.0, 61.3, and 68.2, respectively.

36. An effective interface layer thickness, z_ρ, is introduced through the relation below

$$z_\rho \left(\frac{d S/S_o}{dz} \right)_{max} = 1 \tag{13}$$

where z is positive downward. For the three locations plotted in Figure 25, the values of z_ρ are determined to be 18.52, 20.0, and 13.5, respectively. The ratio, h_1/z_ρ, is then computed to range from 2.05 to 5.05, with the average value being 3.39. Keulegan determined a value of 14.4 in his experiments with fresh water flowing over a stagnant saltwater layer. From Figure 26, which is a plot of field data collected in 1981 at mile 22 and mile 55, the values of h_1/z_ρ are determined to be 4.02 and 6.90, respectively. Therefore, although Keulegan's experiments imply that the numerical results at the

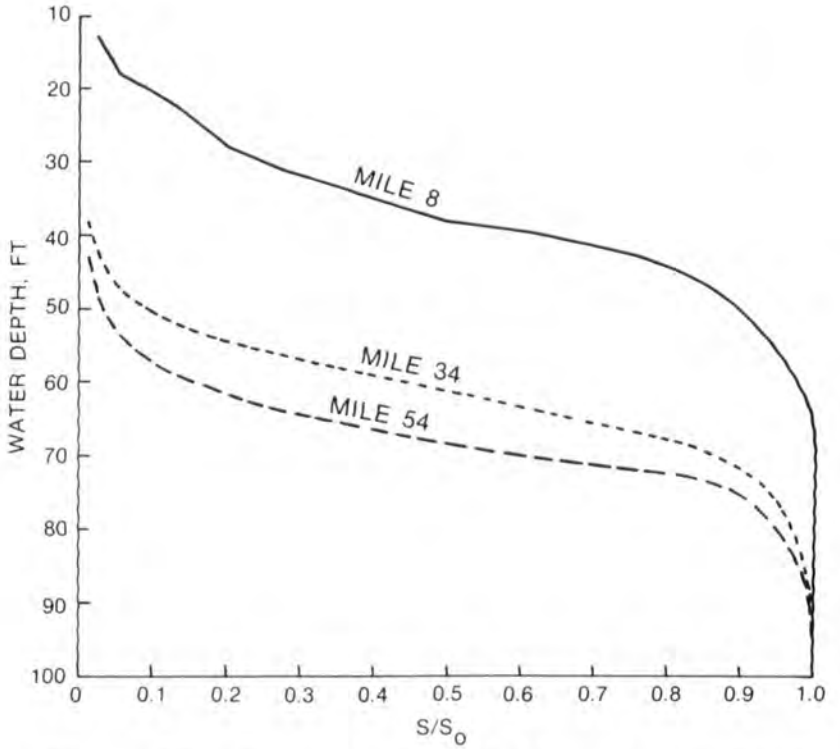

Figure 25. Vertical distribution of normalized salinity computed by LAEM

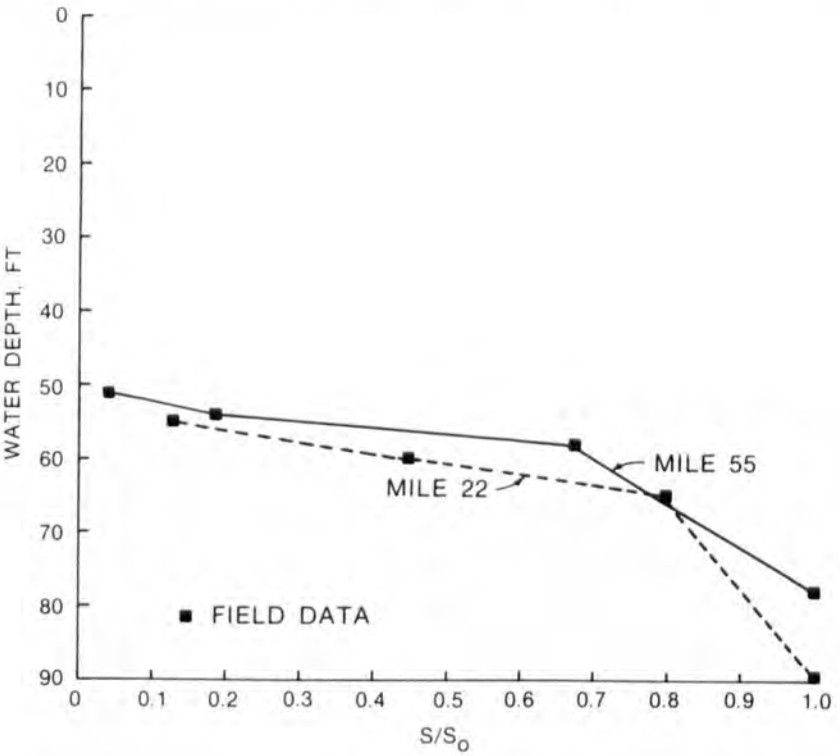

Figure 26. Vertical distribution of normalized salinity from field data

interface are much too diffuse, the limited field data available agree relatively closely with the computed results.

37. The use of z_ρ leads to a dimensionless representation of the salinity. In Figure 27, S/S_o is plotted against the ratio, z'/z_ρ, where z' is the vertical distance from the interface line, for miles 8, 34, and 54. As can be seen, similarity is preserved rather well and the line drawn through the computed data points is the function

$$S/S_o = 1/2 \left(1 - \tanh \frac{2z'}{z_\rho}\right) \tag{14}$$

which is the same function determined by Keulegan (1949).

Distribution of Velocity

38. The vertical distribution of the horizontal component of the flow velocity in the three cross sections at miles 8, 34, and 54 are given in Figure 28, where the ratio of the velocity, U, to the surface velocity, U_s, is plotted against z'/h_1. Although there is some deviation, similarity seems to be somewhat preserved except for the velocity in the saline layer at mile 8. However, it should be noted that the saline layer at mile 8 lies in the hole created by vertical walls at miles 5 and 11 (see Figure 9) and thus might be expected to behave differently.

39. An expression for the representative curve drawn in Figure 28 may be obtained as follows. Since the velocity close to the surface changes slowly, it is assumed that

$$\frac{d(U/U_s)}{d\eta} = (1 - \eta)^2 (a_o + a_1\eta) \tag{15}$$

where

$\eta = z'/h_1$

a_o = value of the rate of change of velocity at $\eta = 0$

a_1 = constant to be determined

From Figure 28, a_o is determined to have a value of 2.5. Integrating, and using the conditions that $U/U_s = 0.25$ at $\eta = 0$ and $U/U_s = 1.0$ at $\eta = 1$, yields

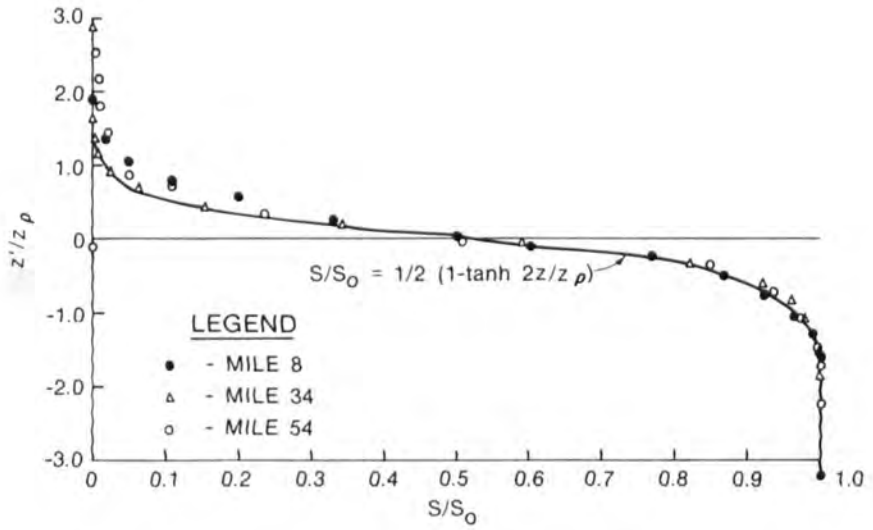

Figure 27. Distribution of normalized salinity about the wedge interface

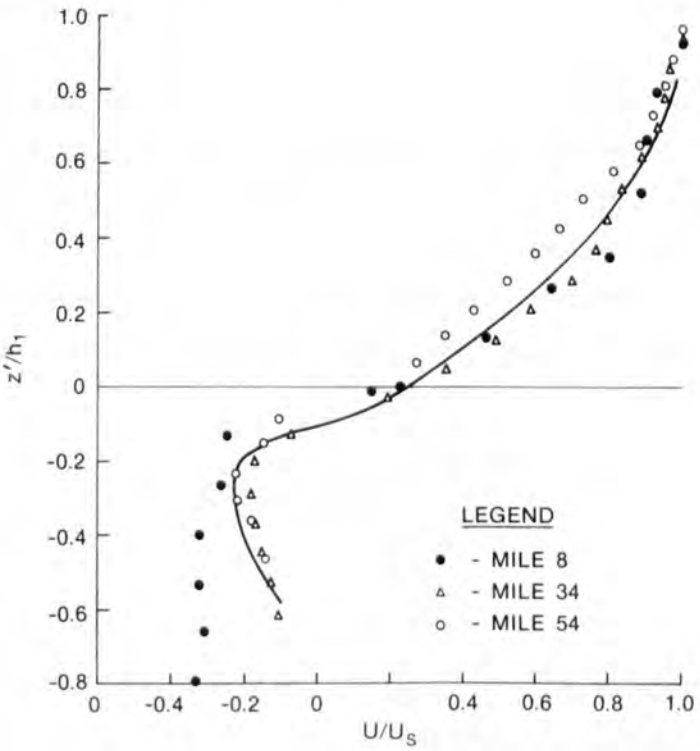

Figure 28. Distribution of normalized longitudinal velocity component about the wedge interface

$$U/U_s = 1/4 + 5/2\eta - 3\eta^2 + 3/2\eta^3 - 1/4\eta^4 \quad (16)$$

Now, using the expression for U/U_s, the average freshwater velocity can be obtained from

$$\bar{U} = \int_0^1 U/U_s \, d\eta \quad (17)$$

to yield

$$\bar{U} = 0.83 \, U_s \quad (18)$$

A numerical integration of the computed freshwater velocities gives

$$\bar{U} = 0.75 \, U_s \quad (19)$$

Therefore the polynomial form for the freshwater velocity seems appropriate.

40. Keulegan's experiments gave a value of $0.54 \, U_s$ for the interfacial velocity, whereas Figure 28 yields a value of $0.25 \, U_s$ for the numerical results. The difference can probably be attributed to the much sharper interface in Keulegan's experiments.

Interfacial Stress

41. Neglecting the momentum of the saline water and sidewall friction effects, Keulegan gives the equation below for the interfacial shear stress, τ_i,

$$\frac{\tau_i}{\rho \bar{U}^2} = \frac{\left(\frac{gh_1}{\bar{U}^2} \frac{\Delta\rho}{\rho} - 1 \right) \frac{dh_2}{dx}}{1 + h_1/h_2} \quad (20)$$

where

$\bar{U}$ = average freshwater velocity

h_1 = depth of the freshwater layer

$\Delta\rho$ = maximum density difference between the saline and fresh water

h_2 = depth of the saline layer.

Figure 29 is a plot of $\Delta\rho/\rho$ versus salinity, as determined from Equation 7, with the water temperature set to 20° C. The first step in the determination of τ_i is the evaluation of dh_2/dx. Since

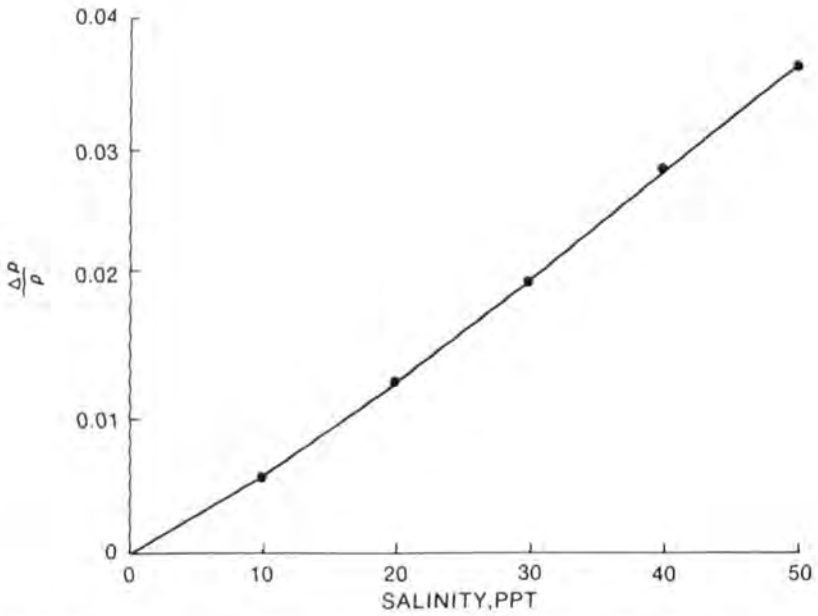

Figure 29. Ratio of excess water density to freshwater density as a function of salinity at a temperature of 20° C

$$100 + \delta = h_1 + h_2 \tag{21}$$

dh_2/dx can be evaluated from

$$dh_2/dx = -dh_1/dx + d\delta/dx \tag{22}$$

where δ is the water-surface elevation above mean sea level. Values of dh_2/dx, where x has been taken as positive in the downstream direction, as well as other variables needed in the evaluation of τ_i are given at various river miles in Table 1. Performing the computations in Equation 20 and averaging over the arrested wedge yields an average value of

$$\left(\frac{\tau_i}{\rho\bar{U}^2}\right)_{avg} = 0.00107 \tag{23}$$

Following Keulegan (1949), the interfacial friction coefficient is defined to be

$$f_i = 8\left(\tau_i/\rho\bar{U}^2\right)_{avg} \tag{24}$$

which yields an average value of $f_i = 0.0086$. However, recall that the interface was defined as that point where the salinity is 1/2 of the bottom salinity

If the value for $\Delta\rho/\rho$ used in the computation for τ_i had been based upon the interface salinity rather than the bottom salinity, the computed value of f_i would have been decreased by a factor of about 2, i.e. the average computed f_i would have been approximately 0.0043.

Critical Flow at the Gulf

42. One important computation for the arrested wedge remains to be made. It is generally assumed that the river mouth is a critical flow section with the densimetric Froude number being equal to unity for the case of highly stratified salt wedges in estuaries. In other words, the average freshwater velocity at the mouth is

$$\bar{U} = \sqrt{\frac{\Delta\rho}{\rho} g h_1} \tag{25}$$

For the case of a constant 150,000-cfs flow, the computed freshwater depth was determined to be 10.39 ft and $\Delta\rho/\rho = 0.024$. Therefore the average freshwater velocity at the river mouth should be 2.83 fps. The numerical results yield an average velocity of 2.53 fps which results in a densimetric Froude number of 0.89. Therefore the numerical results imply that the river mouth is close to being a critical flow section with respect to the densimetric Froude number.

43. The discussion above has been for the purpose of comparing LAEM computed results for an arrested saline wedge with experimental results from Keulegan and known theoretical results. In general, the results compare quite well and serve to increase the credibility of the unsteady results obtained from LAEM that are discussed in PART VI of the report.

PART VI: APPLICATION OF MODEL TO HISTORICAL FLOWS

Steady-Flow Tests

44. An analysis of the impact of a 55-ft channel on salinity intrusion in the Lower Mississippi River was accomplished several years ago by LMN and employed basically a steady-flow approach which assumed a channel of constant width and depth. In the earlier study by Boyd and Johnson (1982), steady-flow tests were run for riverflows of 300,000, 150,000, 125,000, and 91,600 cfs. The last three flows correspond to the low flows experienced during 1980-81, 1963, and 1936, respectively.

45. The 300,000-cfs tests were initiated from a no-flow condition with the flow being increased over a few hours to 300,000 cfs and then held at 300,000 cfs until the wedge position stabilized. Other steady-flow tests were initiated with a flow of 300,000 cfs or less, changed over a few hours to the desired flow, and held there until the wedge position stabilized. The positions at which the wedge stabilized for the different channels and riverflows are plotted in Figure 30 and tabulated below.

	40-ft Channel		55-ft Channel	
Tarbert Landing Discharge, cfs	Wedge Location River Mile	Computation Length, days	Wedge Location River Mile	Computation Length, days
300,000	0	5	11	10
150,000	58	24	92	30
125,000	93	28	116	30
91,600	116	59	127	50

The computed wedge intrusion is generally supportive of the curves developed by LMN (Figure 30), particularly at the lower flows. For the existing 40-ft channel and a riverflow of 91,600 cfs, the wedge was stopped by the Kenner Crossing at mile 116. The computation was run a total of 59 days to make sure that the computation would not ultimately allow the wedge to spill over and move farther upstream. For a proposed 55-ft channel, the wedge was stopped by Kenner Crossing for a discharge of 125,000 cfs. When the discharge was decreased to 91,600 cfs, the wedge did move past the Kenner Crossing but its ultimate position (mile 127) was greatly influenced by the crossing. As noted, these results were obtained from the earlier study in which the additional crossings were not considered. Based upon results from the hydrograph runs

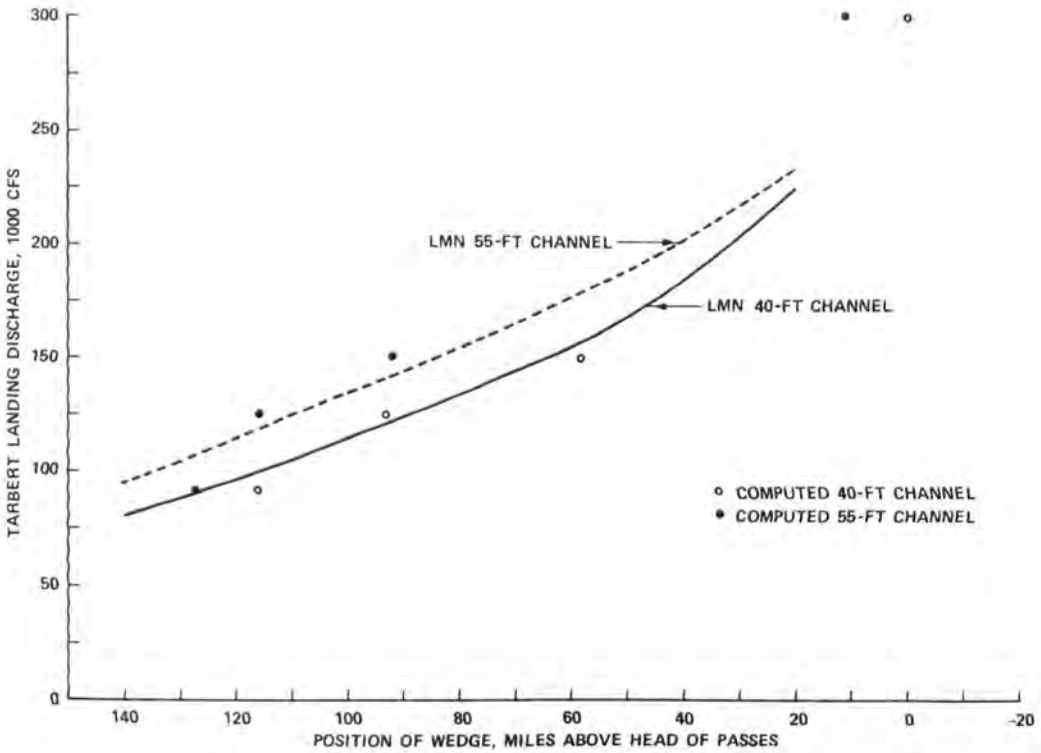

Figure 30. Wedge position for steady-flow tests

discussed next, in which the crossings were considered, essentially the same results would be obtained.

Hydrograph Tests

46. Hydrograph tests were run to provide insight concerning the extent and duration of wedge intrusion for changing riverflow conditions. LMN expressed interest in studying eight low-flow hydrographs which represented a range of frequency of occurrences and shapes. These hydrographs were 1936, 1938-39, 1947-48, 1952-53, 1953-54, 1955-56, 1968, and 1980-81. All hydrographs were initiated from a riverflow of 300,000 cfs with initial conditions that had been saved from a 300,000-cfs steady-state run of the most recently calibrated model containing the additional crossings. Transient solutions were then computed using a time-step of 15 min with recorded Tarbert Landing discharges, lagged by 2 days, prescribed as the upstream boundary condition at Baton Rouge and a zero Gulf elevation as the downstream boundary condition. As previously noted, the downstream salinity boundary condition for all runs was computed from the two profiles presented in Figure 11. The tests for all hydrographs except 1980-81, which of course was used to verify the model,

should be viewed as estimates of how the current and proposed channels would respond to these hydrographs rather than specific simulations of what happened during those periods since no attempt was made to represent channel conditions at those times, e.g., recall the previous discussion in paragraph 14 concerning the shoaling of South Pass since the 1973 flood. However, the general indications should be similar to observations during those periods. Results for each hydrograph tested are summarized in subsequent paragraphs.

47. 1980-81 hydrograph. The low-flow period experienced began in late December 1980 when the river discharge fell below 300,000 cfs on its way to a minimum of about 150,000 cfs and continued into mid-February 1981. The recorded Tarbert Landing hydrograph is shown in Figure 31b. The computed time-histories of corresponding wedge movement for the 40-, 45-, 50- and 55-ft channels are presented in Figure 31a. The maximum intrusion computed during the hydrograph reached approximately the position indicated from the steady-flow tests from the earlier study for the 150,000-cfs flow for both the 40- and 55-ft channel conditions. However, as expected, the time which the wedge was computed to be at that location was significantly less than the time which the flow fluctuated around 150,000 cfs. As noted in the discussion of model calibration, the wedge intrusion for the existing channel is appreciably delayed by the influence of the crossing at mile 47. For the 50- and 55-ft channel, the wedge intrusion is primarily influenced by the crossing at mile 77.

48. 1968 hydrograph. Unlike the 1980-81 hydrograph, the 1968 hydrograph experienced a fall and a subsequent rise back to about 300,000 cfs before moving to its ultimate low flow of about 160,000 cfs. The recorded discharges are given in Figure 32b with the computed wedge movement presented in Figure 32a. The crossing at mile 47 completely stops the computed wedge for the existing and the 45-ft channel. Although this crossing does not appreciably retard the movement of the wedge into the system for the 50- and 55-ft channel, it has a large impact on the movement of the wedge out of the system. The crossing at mile 63 stops the wedge for the 55-ft channel.

49. 1955-56 hydrograph. The computed wedge positions corresponding to the 1955-56 flows on the Lower Mississippi River are shown in Figure 33a, with the discharge hydrograph presented in Figure 33b. With such flows the computed wedge for both a 50- and a 55-ft channel moves past New Orleans (about mile 103) after about 215-220 days. The wedge is stopped by Kenner Crossing

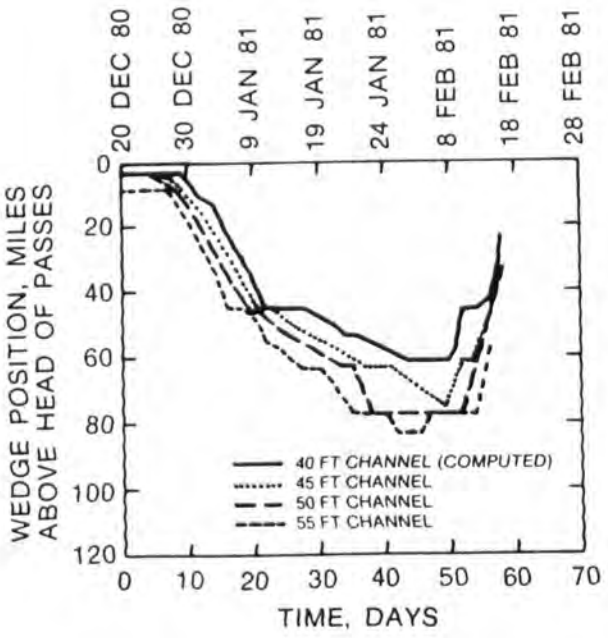

a. Wedge position versus time

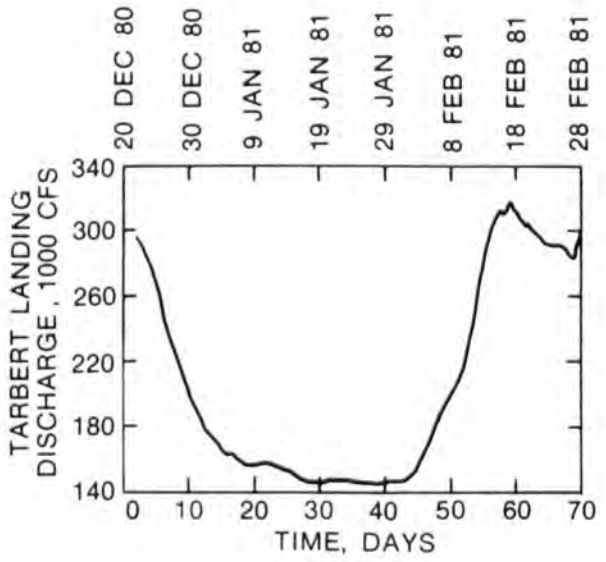

b. Discharge input at Baton Rouge

Figure 31. Results from 1980-81 hydrograph test

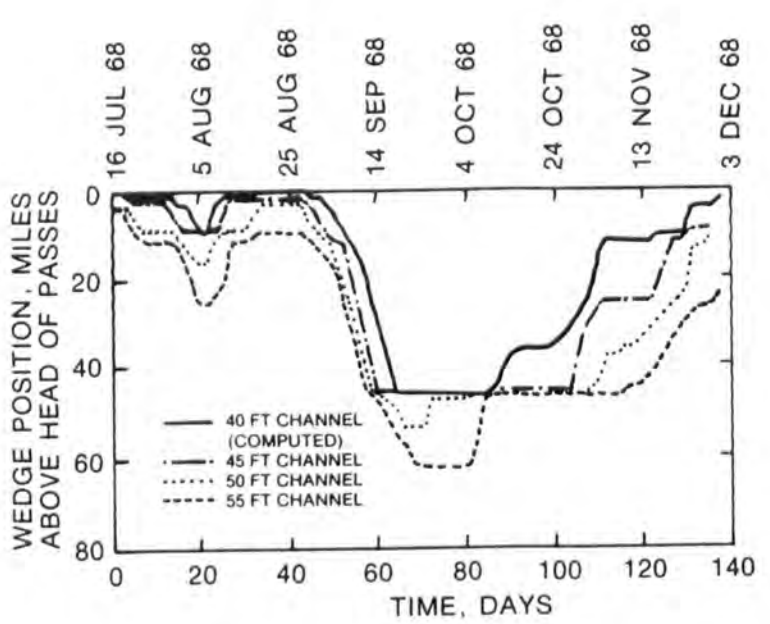

a. Wedge position versus time

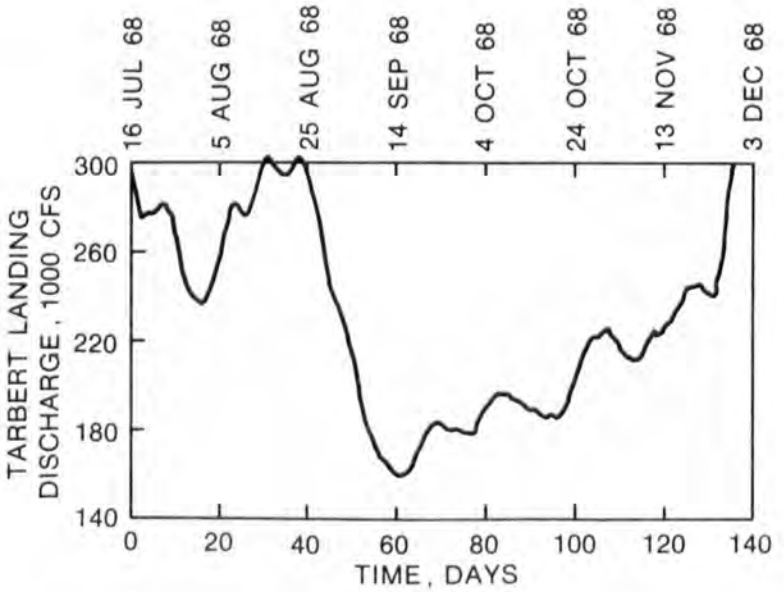

b. Discharge input at Baton Rouge

Figure 32. Results from 1968 hydrograph test

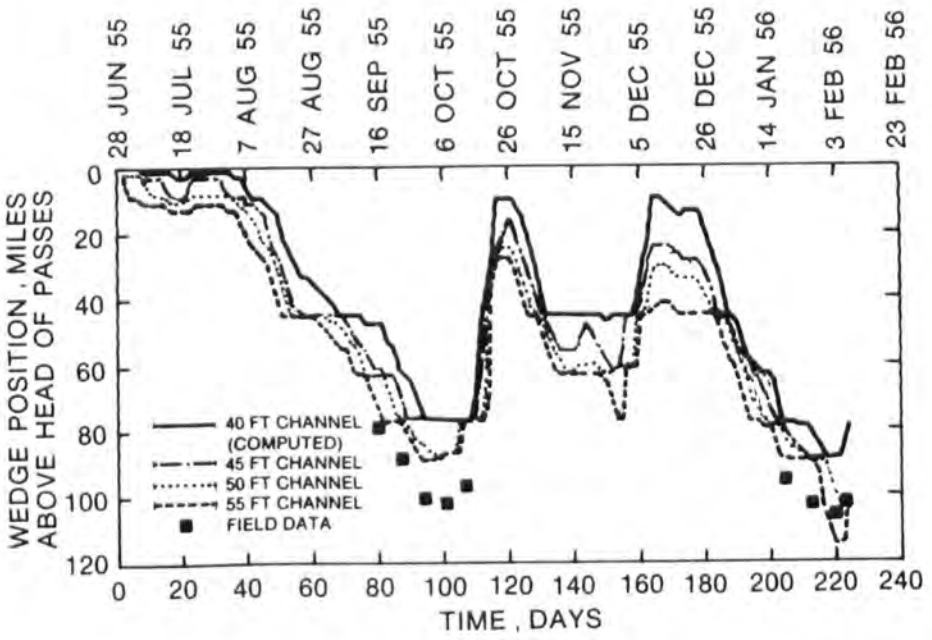

a. Wedge position versus time

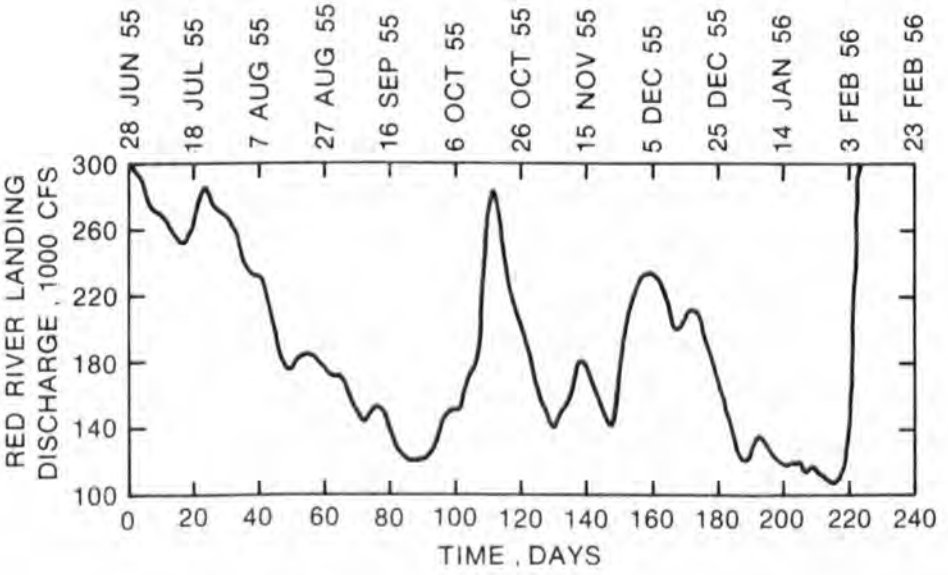

b. Discharge input at Baton Rouge

Figure 33. Results from 1955-56 hydrograph test

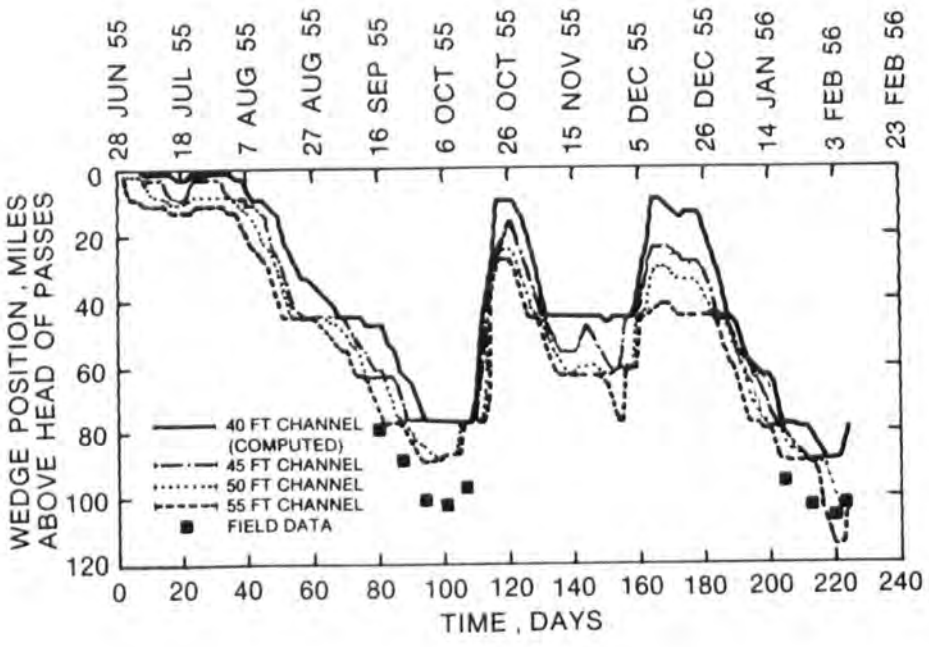

a. Wedge position versus time

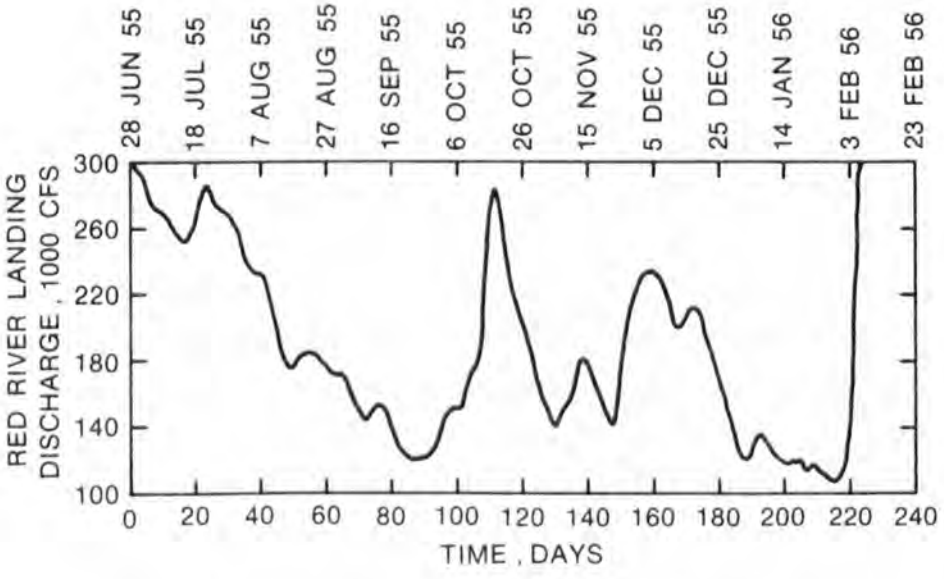

b. Discharge input at Baton Rouge

Figure 33. Results from 1955-56 hydrograph test

at mile 116. As can be seen, the wedge computed with the existing 40-ft channel does not match the field data. However, again it should be remembered that the channel conditions which currently exist below the Head of Passes are quite different from those that existed in 1955-56. Therefore one should not expect the computed wedge for existing conditions to match the field data. Figure 34 presents wedge profiles along the river for both the 40- and 55-ft channels at a time when the concentrations are at their highest point in the water column at New Orleans.

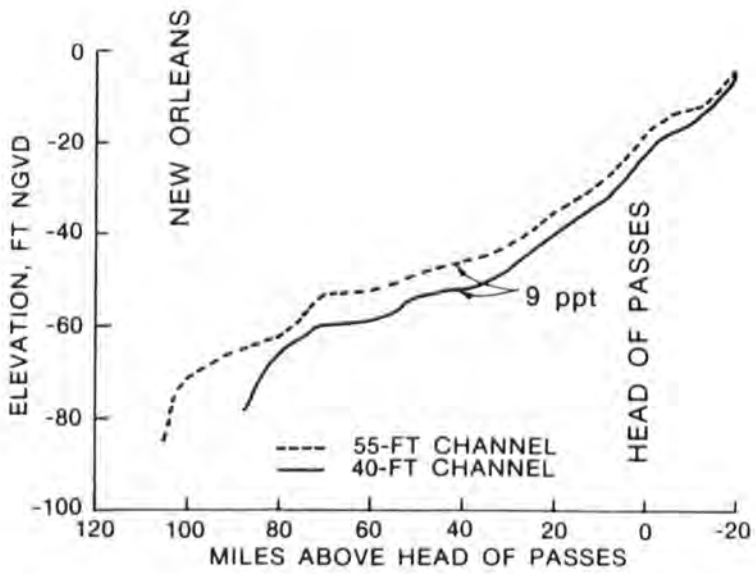

Figure 34. Wedge interfaces at the time of minimum wedge depth at New Orleans during the 1955-56 computations

50. 1953-54 hydrograph. The 1953-54 hydrograph presented in Figure 35b resembles the 1980-81 hydrograph but with a lower flow that is maintained for a much longer period of time. As shown in Figure 35a for the wedge movement, the crossings at miles 47, 63, and 77 have a relatively minor effect on the intrusion of the wedge even for the 40-ft channel. Kenner Crossing at mile 116 completely stops the wedge for all channels. Figure 36 presents wedge profiles along the river at a time when the concentrations are at their highest point in the water column at New Orleans. An interesting observation is that the computed wedge for the 55-ft channel comes quite close to matching the field data. One might be tempted to conclude that deepening Southwest Pass to 55 ft impacts the intrusion of the wedge about as much as if both South Pass and Pass a Loutre were restored to their 1953-54 conditions. One

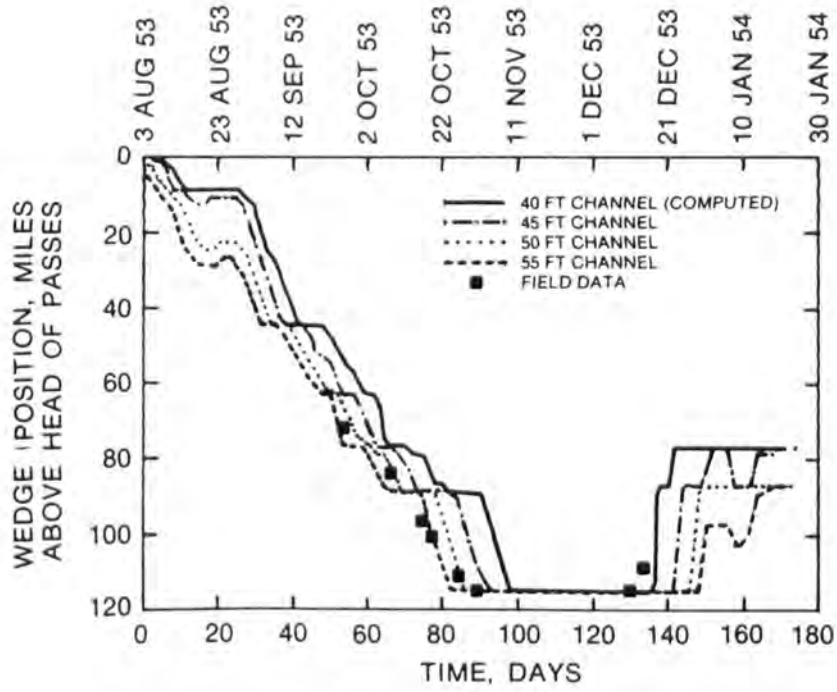

a. Wedge position versus time

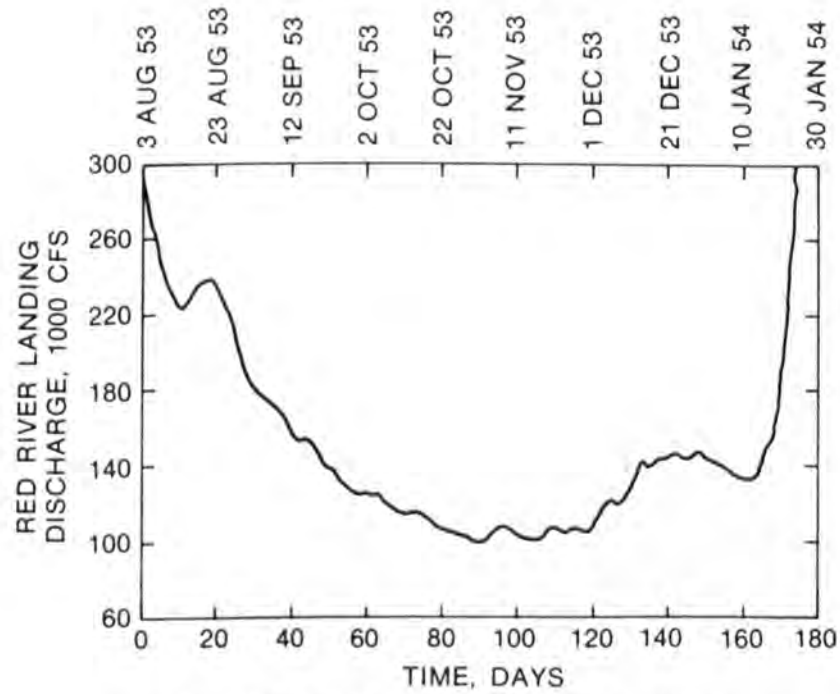

b. Discharge input at Baton Rouge

Figure 35. Results from 1953-54 hydrograph test

way to substantiate this would be to employ a recently developed version of LAEM that has a branching capability. However, since this would constitute a substantial modeling effort, arrested wedge computations were made instead in an attempt to provide some insight.

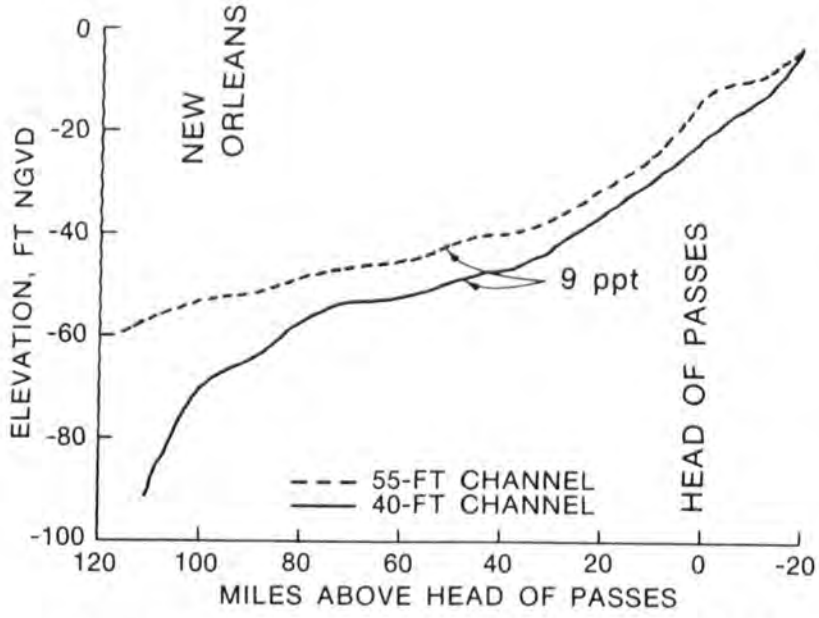

Figure 36. Wedge interfaces at the time of minimum wedge depth at New Orleans during the 1953-54 computations

51. These computations were made by solving a continuity equation for the flow in the upper freshwater layer, i.e.,

$$\frac{duh_1B}{dx} = Q_e \tag{26}$$

and momentum equations for both the freshwater layer and the stationary bottom saline layer, i.e.,

$$\frac{d\left(h_1 + h_2\right)}{dx} + \frac{u}{g}\frac{du}{dx} - \frac{\tau_i}{\gamma h_1} - S_o = 0 \tag{27}$$

$$\left(1 - \frac{\Delta\rho}{\rho}\right)\frac{dh_1}{dx} + \frac{dh_2}{dx} + \frac{\tau_i}{\gamma h_2} - S_o = 0 \tag{28}$$

with the x-axis drawn in the opposite direction of freshwater flow. Variables in the equations are defined as:

u = mean freshwater velocity, fps

h_1 = depth of freshwater layer, ft

B = channel width, ft

Q_e = lateral outflow per unit length, $ft^3/s/ft$

h_2 = depth of saline layer, ft

g = acceleration due to gravity, ft/s^2

τ_i = interfacial shear, $lbm/ft/s^2$

γ = mean specific weight for fresh and salt water, $lbm/ft^2/s^2$

S_o = bottom slope, ft/ft

$\Delta\rho$ = differential density between fresh and salt water, lbm/ft^3

ρ = density of fresh water, lbm/ft^3

These equations have been taken from Schijf and Schonfeld (1953). Writing the interfacial shear stress as

$$\tau_i = \frac{\rho f_i}{8} u^2 \tag{29}$$

where f_i is a nondimensional interfacial friction factor, combining Equations 27 and 28 and replacing the derivatives in the equations by centered differences results in

$$u^{i+1} = u^i \frac{h_1^i B^i}{h_1^{i+1} B^{i+1}} + \frac{Q_\ell^i \Delta x}{h_1^{i+1} B^{i+1}} \tag{30}$$

$$h_1^{i+1} = h_1^i - \frac{u^{i+1} + u^i}{2g\Delta\rho/\rho} (u^{i+1} - u^i)$$

$$+ \frac{f_i \left(u^{i+1} + u^i\right)^2 \Delta x}{16g\Delta\rho/\rho} \left(\frac{1}{h_1^{i+1} h_1^i} + \frac{1}{h_2^{i+1} + h_2^i} \right) \tag{31}$$

To solve these equations, the freshwater discharge upstream of the wedge must be specified and densimetric critical flow is specified at the river mouth, i.e.,

$$\frac{u}{\sqrt{g h_1 \frac{\Delta\rho}{\rho}}} = 1 \tag{32}$$

The solution of Equations 30 and 31 is an iterative one in that u^{i+1} is obtained by guessing at h_1^{i+1}. This value of u^{i+1} is then used to compute a value for h_1^{i+1} which in turn is used to recompute u^{i+1}. This process continues until the value of h_1^{i+1} converges within some specified tolerance, e.g. 0.01 ft. These computations are patterned after Balloffet and Borah (1985).

52. Two cases were computed. The first is illustrated below.

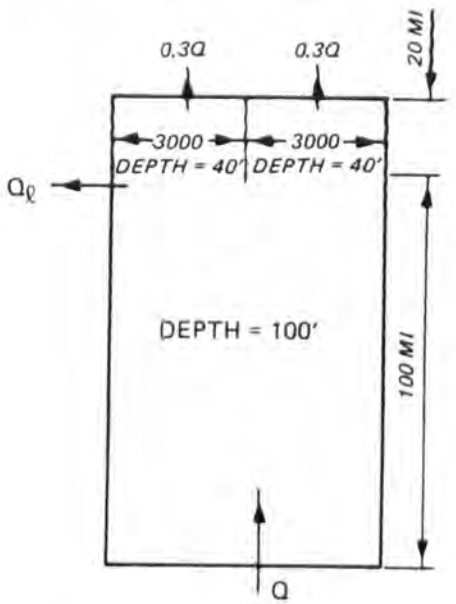

Here it is assumed that two identical channels with widths of 3,000 ft and depths of 40 ft lead to the ocean. Each channel carries 30 percent of the total riverflow. As shown below, the second case is for a single 55-ft channel leading to the ocean and also carrying 30 percent of the total flow. Using values of $(\Delta\rho/\rho) = 0.02$ and $f_i = 0.003$ and an assumed water-surface

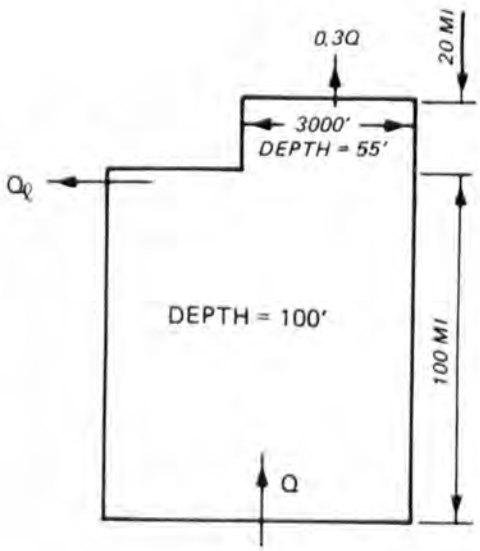

profile representative of the lower Mississippi River, arrested saline wedges were computed for freshwater discharges of 150,000 and 100,000 cfs. At 70 miles from the ocean end, the freshwater depth was computed to be about 5 ft greater with the two 40-ft channels when the river discharge was 150,000 cfs. However, with a discharge of 100,000 cfs the freshwater depth at the same location was computed to be only about 1 ft greater with the two 40-ft channels. The general conclusion then, based upon arrested saline wedge theory, is that as the river discharge decreases, the salt wedge created by two 40-ft channels approaches the wedge created by a single 55-ft channel. In other words, arrested saline wedges created as a result of extremely low riverflow for channel conditions simulating those before 1973 were approximately of the same strength as those that would be created by a 55-ft channel in Southwest Pass today under the same flow conditions.

53. A comment at this time on how the tip of the wedge is determined as the riverflow increases and forces the wedge back toward the Gulf is in order. For consistency, when the salinity concentration drops below 9 ppt in a column of computational cells the wedge tip is considered to be located in the adjacent downstream column. Since concentrations on top of the crossings are the first to fall below 9 ppt, jumps can be seen in wedge position plots (for example, day 148 of the 55-ft channel curve in Figure 35a). This is further illustrated in Figure 37 where plots of the 9-ppt interface on two different days are presented.

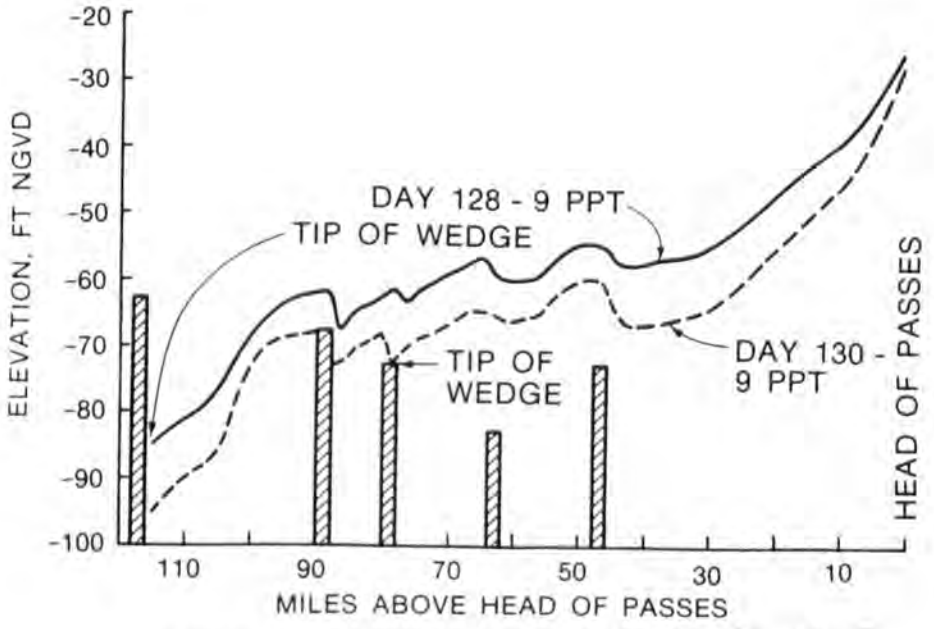

Figure 37. Determination of the wedge tip

54. 1952-53 hydrograph. The minimum flow in the 1952-53 hydrograph presented in Figure 38b is about 115,000 cfs and lasted for about 35 days. As a result, the computed wedge for all channels (Figure 38a) moved past New Orleans to Kenner Crossing, with the wedge from the deepened channels remaining there much longer. Plots of the 9-ppt profiles for both the 40- and 55-ft channels are given in Figure 39 at the time of the minimum depth of the wedge interface at New Orleans.

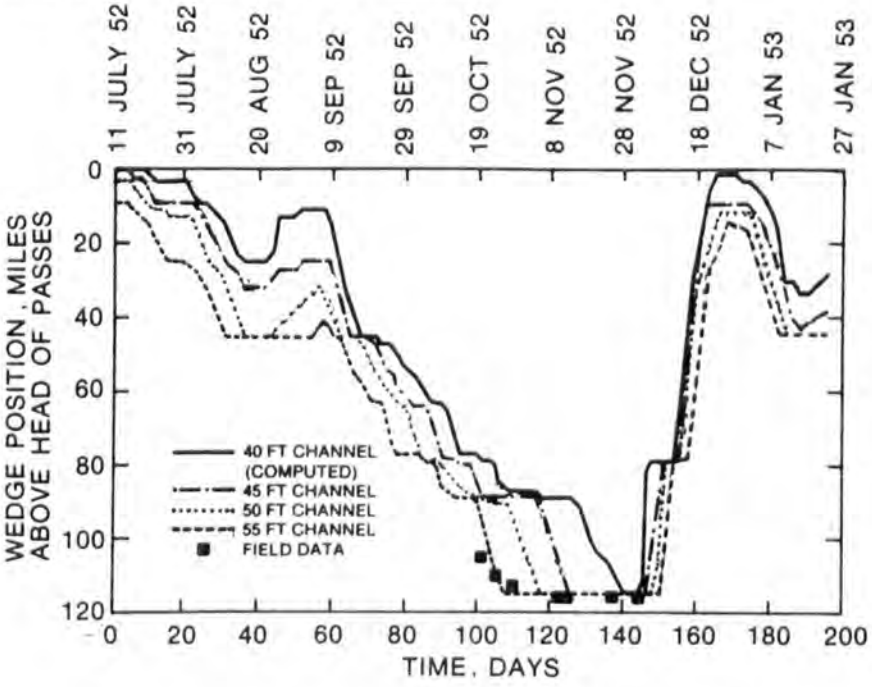

a. Wedge position versus time

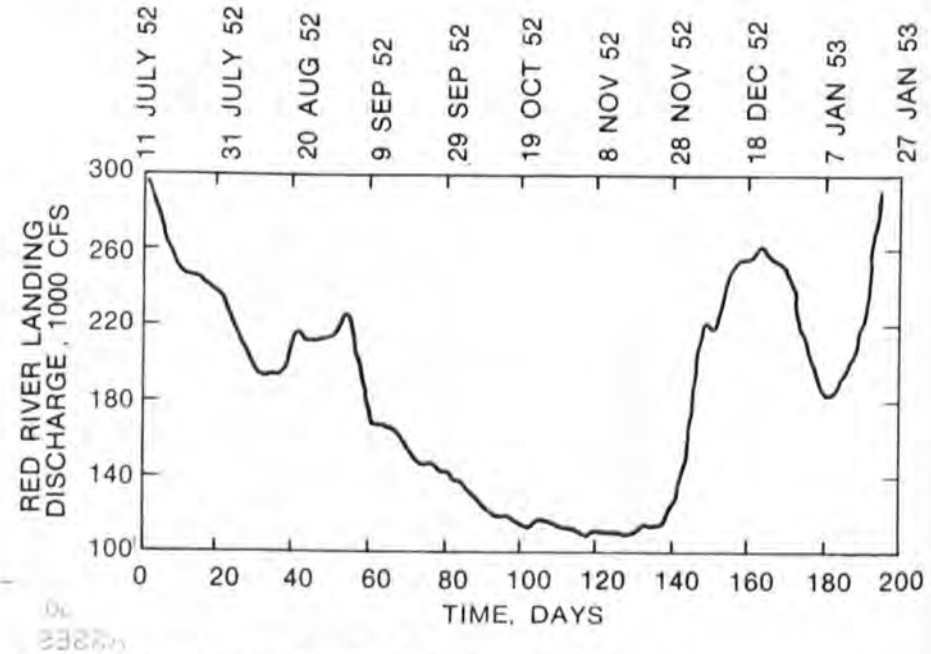

b. Discharge input at Baton Rouge

Figure 38. Results from 1952-53 hydrograph test

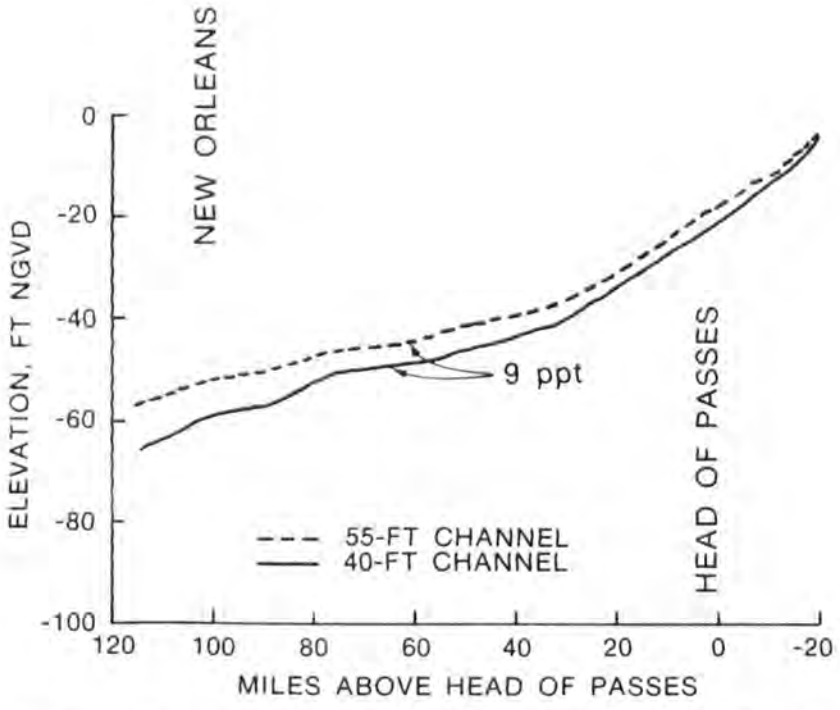

Figure 39. Wedge interfaces at the time of minimum depth at New Orleans during the 1952-53 computations

55. 1947-48 hydrograph. The 1947-48 hydrograph contains a relatively smooth fall from 300,000 cfs to a low of about 120,000 cfs over a period of 90 days with a subsequent rise to 220,000 cfs over the next 30 days (Figure 40b). As plotted in Figure 40a, the crossing at mile 47 retards the wedge in the 40-ft channel for about 25 days with subsequent intrusion to the crossing at mile 87 where it remains until the flow increases enough to move it back toward the Gulf. However, for the 55-ft channel, the computed wedge moves past New Orleans with about a 5- to 10-day retardation period at each of the crossings. Wedge profiles along the river are presented in Figure 41.

56. 1938-39 hydrograph. The 1938-39 hydrograph plotted in Figure 42b represents a rapidly varying flow between a high of 300,000 cfs and a low of 140,000 cfs. The maximum extent of the computed wedge for the 45-, 50- and 55-ft channels is the crossing at mile 77 (Figure 42a). The major interest in this hydrograph is in the rapid manner in which the wedge for both the existing and the deepened channels responds to the rapidly varying flow during the series of rises and falls that occur.

57. 1936 hydrograph. The low flow experienced in 1936 extended over a rather lengthy period with flow dropping below 300,000 cfs in early June on its way to a minimum flow of 91,600 cfs some 95 days later (Figure 43b). The

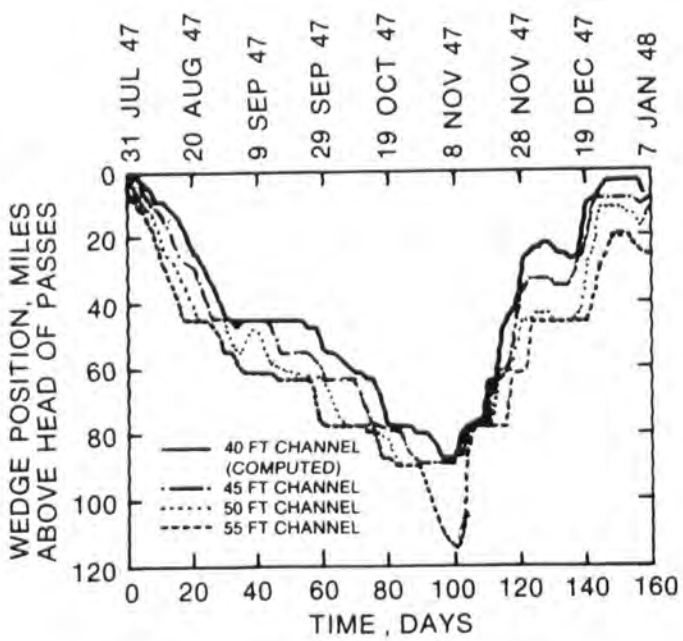

a. Wedge position versus time

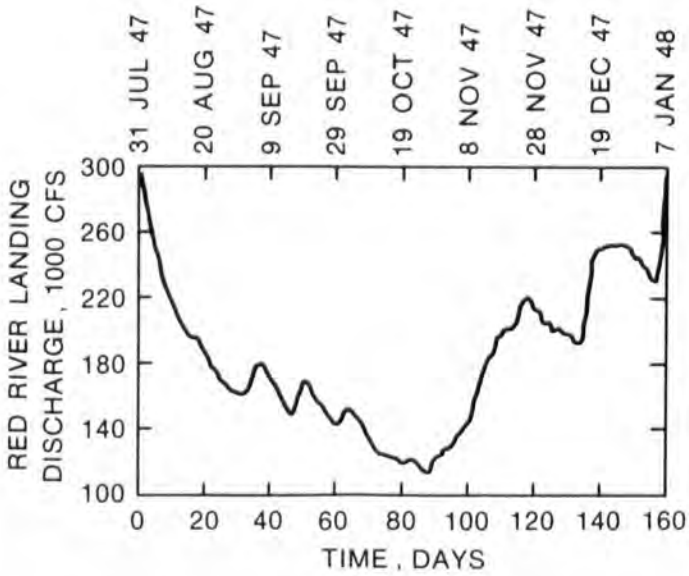

b. Discharge input at Baton Rouge

Figure 40. Results from 1947-48 hydrograph test

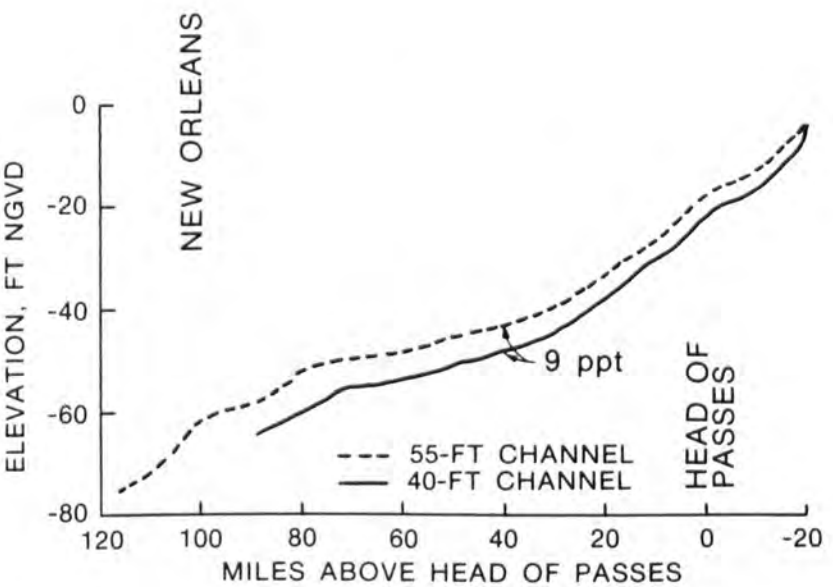

Figure 41. Wedge interfaces at the time of minimum wedge depth at New Orleans during the 1947-48 computations

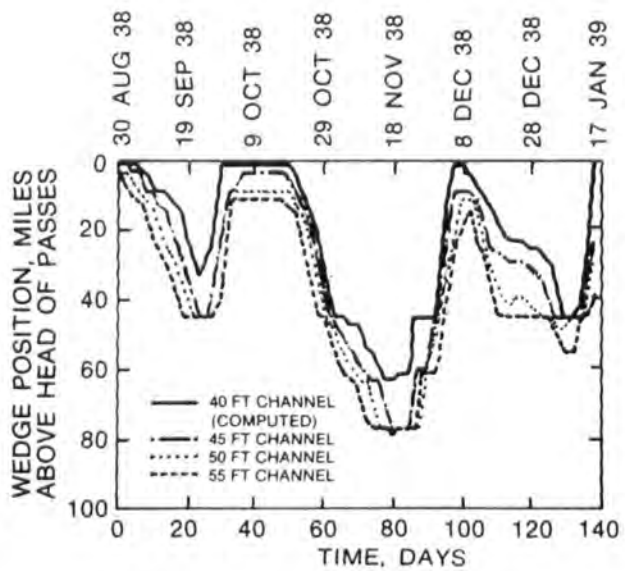

a. Wedge position versus time

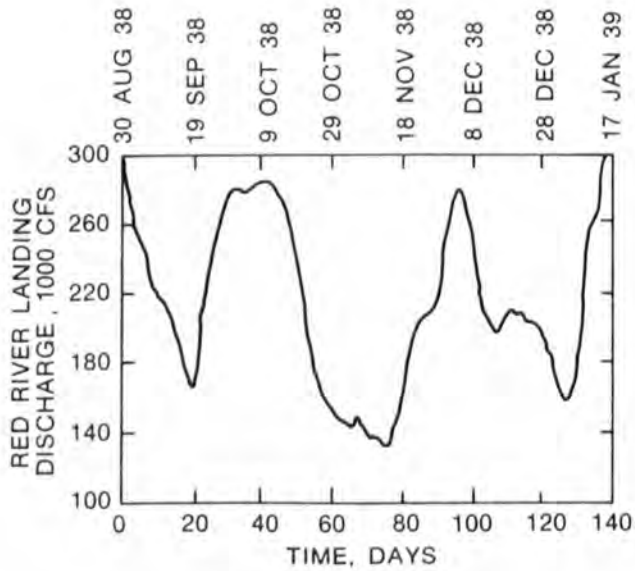

b. Discharge input at Baton Rouge

Figure 42. Results from 1938-39 hydrograph test

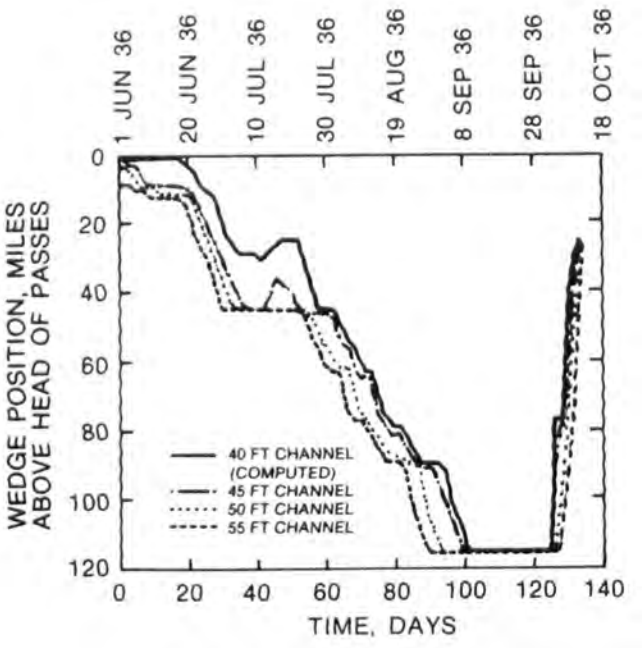

a. Wedge position versus time

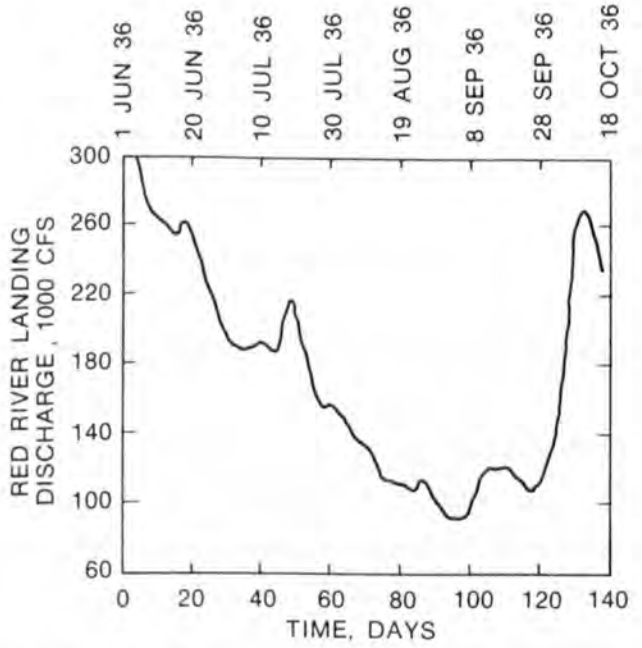

b. Discharge input at Baton Rouge

Figure 43. Results from 1936 hydrograph test

computed wedge movements in response to the 1936 hydrograph are plotted in Figure 43a. The maximum intrusion for all channels is Kenner Crossing. The effect of the crossing at mile 47 on the wedge is clearly evident. As previously discussed in paragraph 53, Figure 37 illustrates the manner in which

the tip of the wedge is determined. The primary wedge for the 1936 hydrograph moves out rapidly but pockets of high-salinity water are temporarily trapped on the upstream side of channel crossings. Figure 44 presents a plot of the 9-ppt profiles for both the 40 and 55-ft channels.

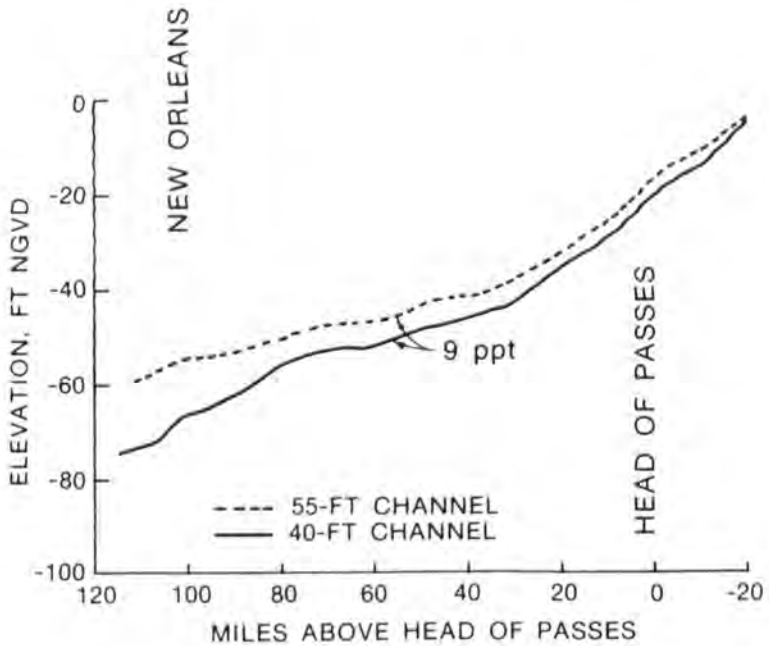

Figure 44. Wedge interfaces at the time of minimum wedge depth at New Orleans during the 1936 computations

Duration Results

58. These hydrograph tests provide information on the extent of the wedge intrusion for the 40-, 45-, 50-, and 55-ft channels under a wide range of flow hydrographs that have occurred in the past. In addition, results from the tests can be used to estimate the duration of wedge intrusion, based upon a concentration of 9 ppt, beyond Port Sulphur (mile 40), Algiers (mile 96), and New Orleans (mile 103). Increases in duration as a result of the deepened channels are presented in Tables 2-4. Figures 45 and 46 contain plots for both the 40- and 55-ft channels of duration of wedge intrusion versus river miles for the 1953-54 and 1936 hydrographs, respectively. The influence of the various river crossings is responsible for the sharp changes in slope on some of the curves. For the 55-ft channel, the 1953-54 hydrograph results in a wedge that stays past New Orleans for 67 days (Figure 35a or Figure 45). The conditions at New Orleans generated by the 1952-53 (Figure 38a) and the

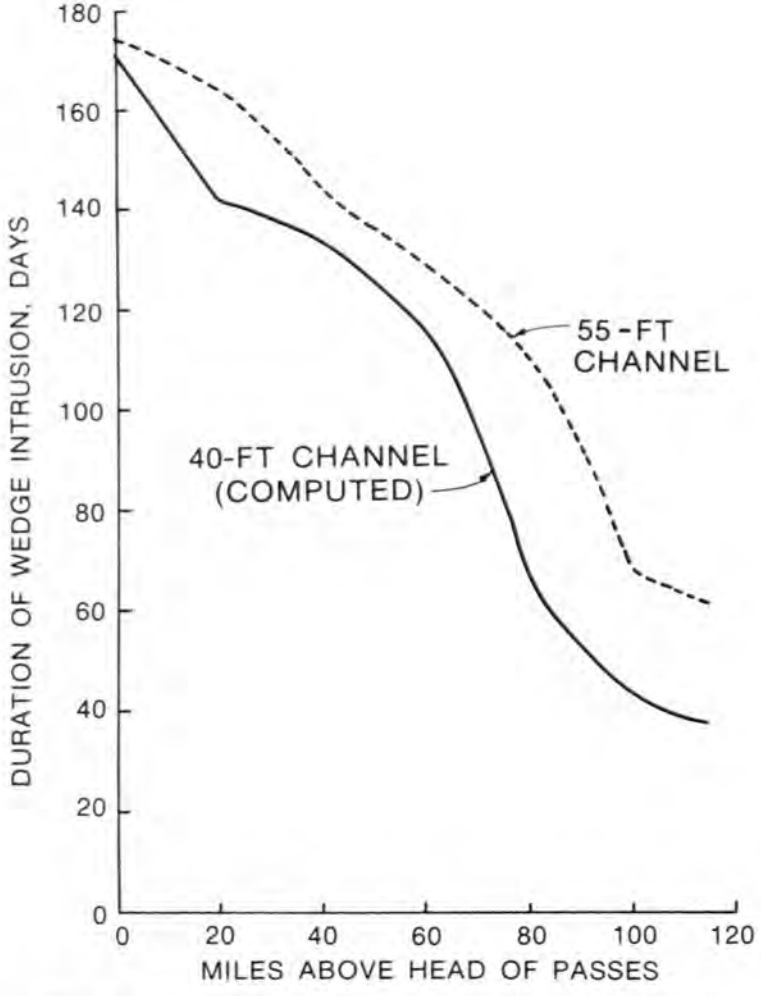

Figure 45. Duration of wedge intrusion for 1953-54 hydrograph test

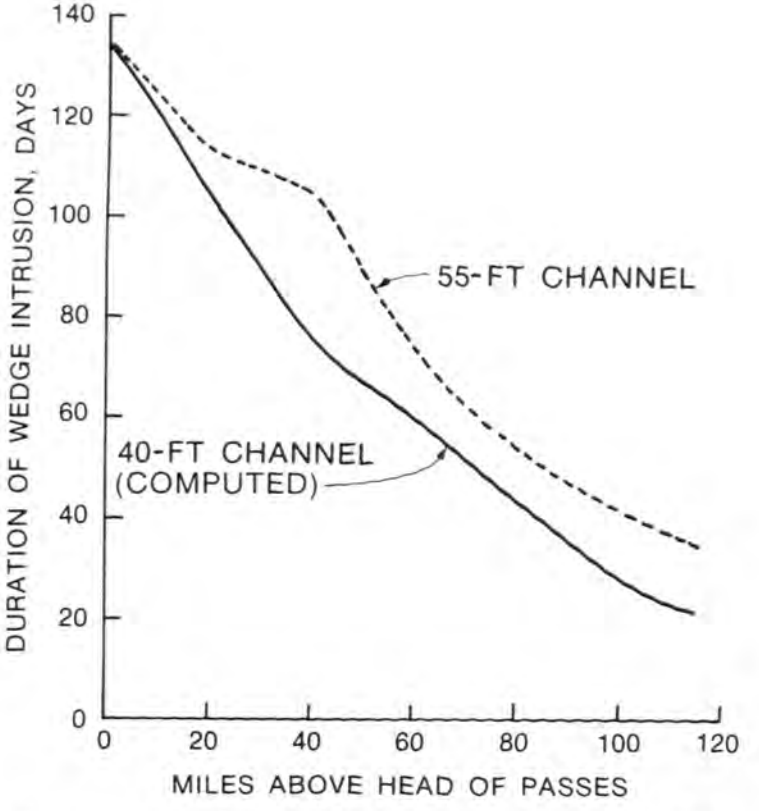

Figure 46. Duration of wedge intrusion for 1936 hydrograph test

1936 (Figure 43a or Figure 46) hydrographs for a 55-ft channel appear to be of approximately equal severity, with the wedge remaining past New Orleans for about 40 days. Hydrographs such as the 1980-81, 1968, and 1938-39 would not create problems for locations beyond the crossing at mile 77.

PART VII: SILL TESTS

59. Results from the hydrograph tests reveal that deepened channels up to 55 ft will significantly increase the extent and duration of salinity intrusion. As a possible means of either stopping or at least severely retarding the intrusion of the salt wedge during critically low-flow periods, a sill constructed from bed material that is primarily fine sand has been proposed at the crossing located at about mile 63. The sill would have a triangular shape with 1V on 40H side slopes and a maximum top elevation of -55 ft. The stability of the increased height of the crossing was determined using the HEC-6 computer program "Scour and Deposition in Rivers and Reservoirs" (HEC 1977); whereas its impact on the extent of salinity intrusion was of course determined by employing the flow-salinity model, LAEM. The sill stability tests were conducted by Copeland (1983), and the following discussion was taken from his summary of the results of the computer runs.

Sill Stability

60. The study reach extended from Venice, at river mile 10.7, to New Orleans, at river mile 102.7. An HEC-6 model set up by LMN was used as a base for geometric and bed material data. Additional cross sections were taken from the 1973-75 hydrographic survey. The Toffaleti sediment transport function was used in the model because it favorably reproduced sediment measurements from Tarbert Landing (river mile 316). Sediment input into the numerical model was initially determined from calculated hydraulic parameters. The sediment input was adjusted to maintain an essentially stable bed elevation at the upstream cross section. Cross sections identified as erosion-resistant were not allowed to erode in the numerical model. A report by Kolb (1963) was used to make these determinations. The downstream water-surface rating curve was determined from daily stages at Venice and discharges routed from Tarbert Landing and Carrollton. Hydrographs were developed from daily discharge records at Tarbert Landing and were limited to a maximum of 1,250,000 cfs; this accounted for operation of the Bonne Carre and Morganza Floodways. The Pointe a la Hache Relief Outlet, located between river miles 33 and 44, allows some flow to leave the river when the water-surface elevation exceeds 7 ft. At a maximum discharge of 1,250,000 cfs, LMN estimated

that the outflow would only be about 30,000 cfs or 2 percent of the total. The effect of the outlet was considered insignificant and was therefore not simulated in the study.

61. The numerical flow model was verified by matching recorded stages at eight gages for a range of steady-state discharges. This was accomplished by adjusting Manning's roughness coefficients. Adopted values varied with discharge and ranged between 0.013 and 0.028 from Venice to river mile 50 and between 0.020 and 0.035 from river mile 50 to New Orleans. Calculated water-surface elevations compared favorably with measured stages as shown in Figure 47.

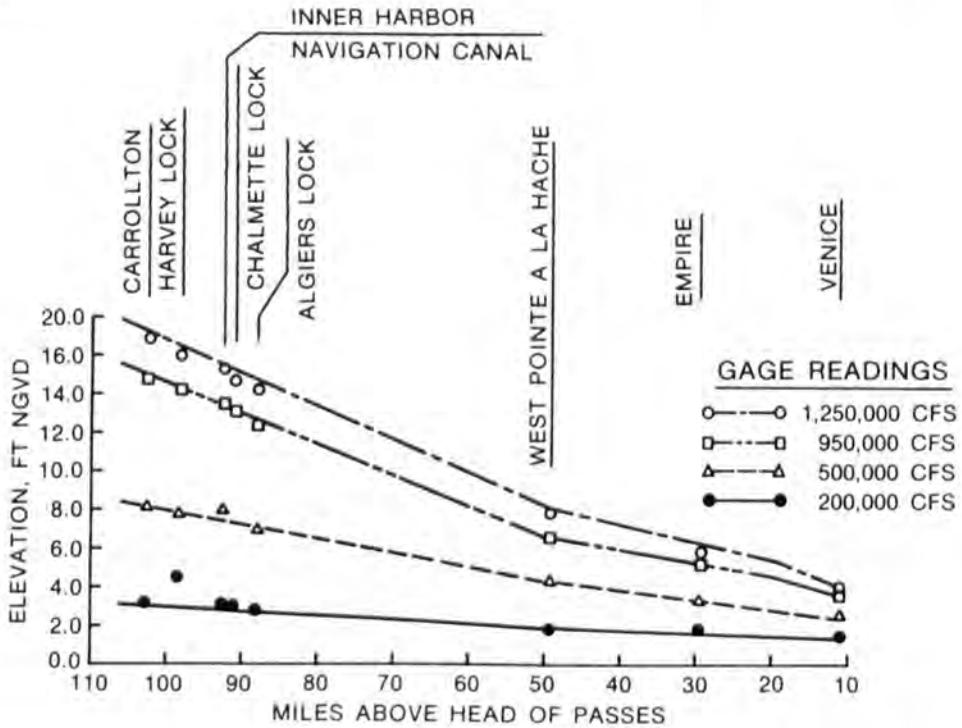

Figure 47. Water-surface profiles from HEC-6 model

62. The sediment model was verified by comparing measured and calculated sediment transport rates and bed changes. Calculated transport rates at river mile 76 compared favorably with measured values at the Belle Chase gage (Figure 48). Data from the 1963-65, 1973-75, and 1982 hydrographic surveys indicated that bed elevations in the study reach did not change significantly. Eight years of record (1975-1982) were simulated in the model; bed changes in the vicinity of the sill were insignificant (Figure 49). The model was not sufficiently verified below river mile 50 where significant scour and

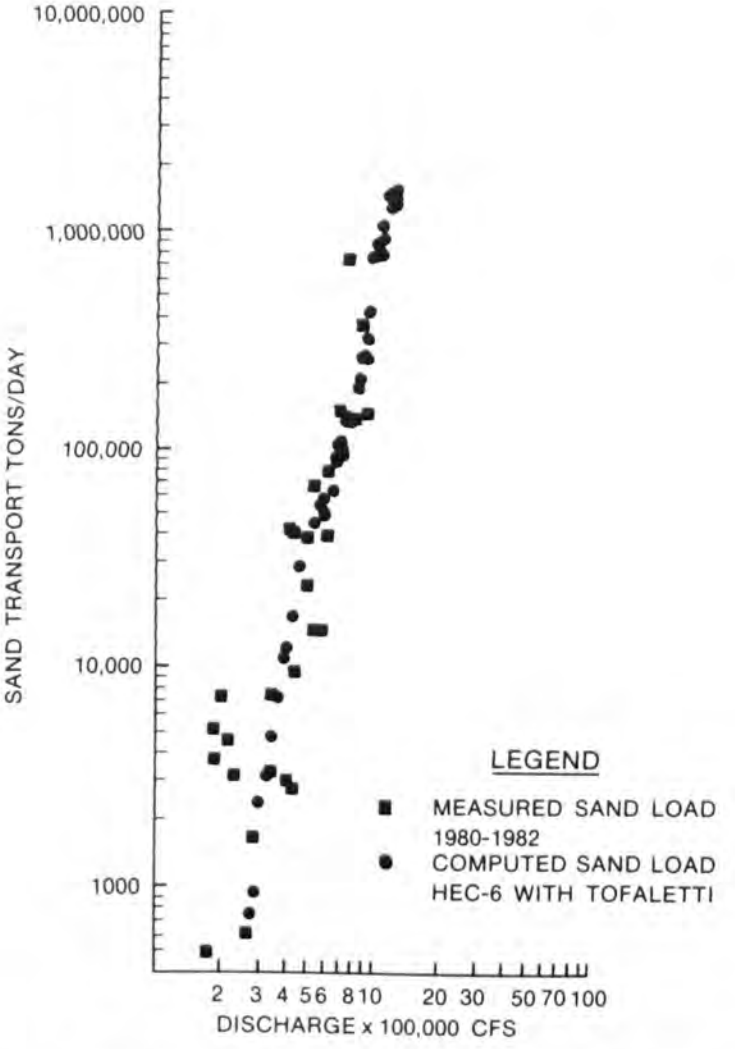

Figure 48. Sediment discharge at Belle Chase gage located at mile 76.0

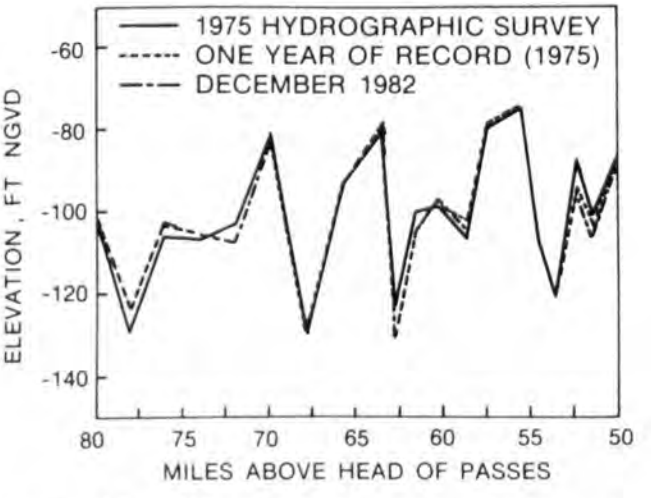

Figure 49. Mississippi River thalweg in vicinity of proposed sill

deposition were calculated, but these results did not affect the calculations in the area of interest.

63. The verified numerical model was used to determine the stability of the sill. Steady-state discharges ranging between 200,000 and 800,000 cfs were simulated for a period of 150 days; the following depths were eroded off the top of the sill:

Discharge, cfs	Erosion, ft
200,000	0.02
300,000	1.4
400,000	2.0
450,000	5.0

Rates of erosion for higher discharges are shown in Figure 50. At a discharge of 800,000 cfs, the sill washed out in about 5 days. The sill may be considered stable when the discharge is less than 400,000 cfs.

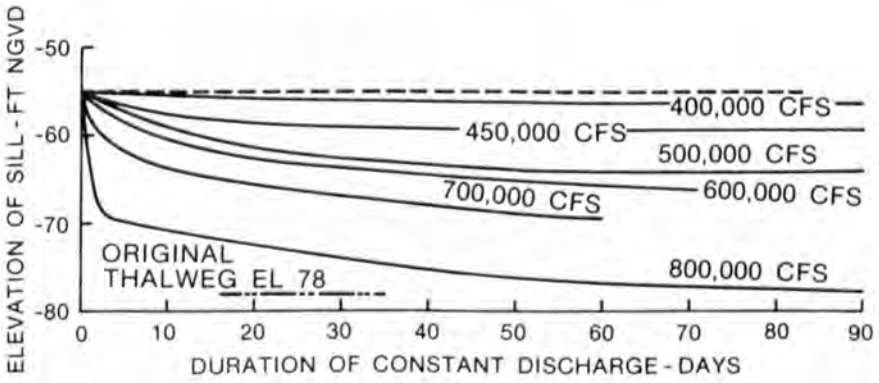

Figure 50. Erosion of triangular sill (1V on 40H) at mile 63.4

Impact of Sill on Salinity Intrusion

64. Of all the hydrographs tested, the 1953-54 hydrograph produced the most severe salinity conditions at New Orleans, although the low flow of record occurred in 1936 and historical records imply that salinity conditions were more severe in 1936. However, again it should be remembered that channel conditions in 1936 and 1953 were probably not the same, whereas, the same channel was used in the model for all runs. In addition, values for the recorded river flows employed could be in error by as much as perhaps 10-15 percent. Therefore the 1953-54 flow conditions at Baton Rouge, as well as the

1936 conditions, were used to test the effect of various sills at mile 63 on salinity intrusion. The wedge intrusion for a sill height of -55 ft is presented in Figures 51 and 52 for the 1953-54 conditions and 50- and 55-ft channels, respectively. A similar plot for a 45-ft channel but with the sill at -60 ft is presented in Figure 53. Likewise, the wedge intrusion for a sill height of -55 ft is presented in Figures 54 and 55 for the 1936 conditions and 50- and 55-ft channels, respectively. A similar plot for a 45-ft channel and sills at heights of -65, -60, and -55 ft is presented in Figure 56. Although a sill does not completely stop the wedge, the movement of the wedge is retarded such that the overall intrusion with the -55-ft sill in a 55-ft channel closely follows that computed with the 40-ft channel. Decreases in duration beyond Port Sulfur, Algiers, and New Orleans, as a result of a -55-ft sill in a 55-ft channel, are presented in Table 5.

Effect of Sill Discretization on Salinity Intrusion

65. As discussed in paragraph 18, the earliest runs of LAEM utilized a spatial step of 1 mile, whereas the runs discussed here employed a Δx of 2 miles in the geometric representation of the system. Therefore a sill constructed on the natural crossing at mile 63 is assumed to be 2 miles wide. The question of the effect of the width of the sill on salinity intrusion has been posed. Based upon the fact that essentially no differences in the computations were observed between runs in which river crossings were represented by 1 mile and then 2 miles, it is not believed that the width of the sill has an appreciable effect on the flow-salinity fields.

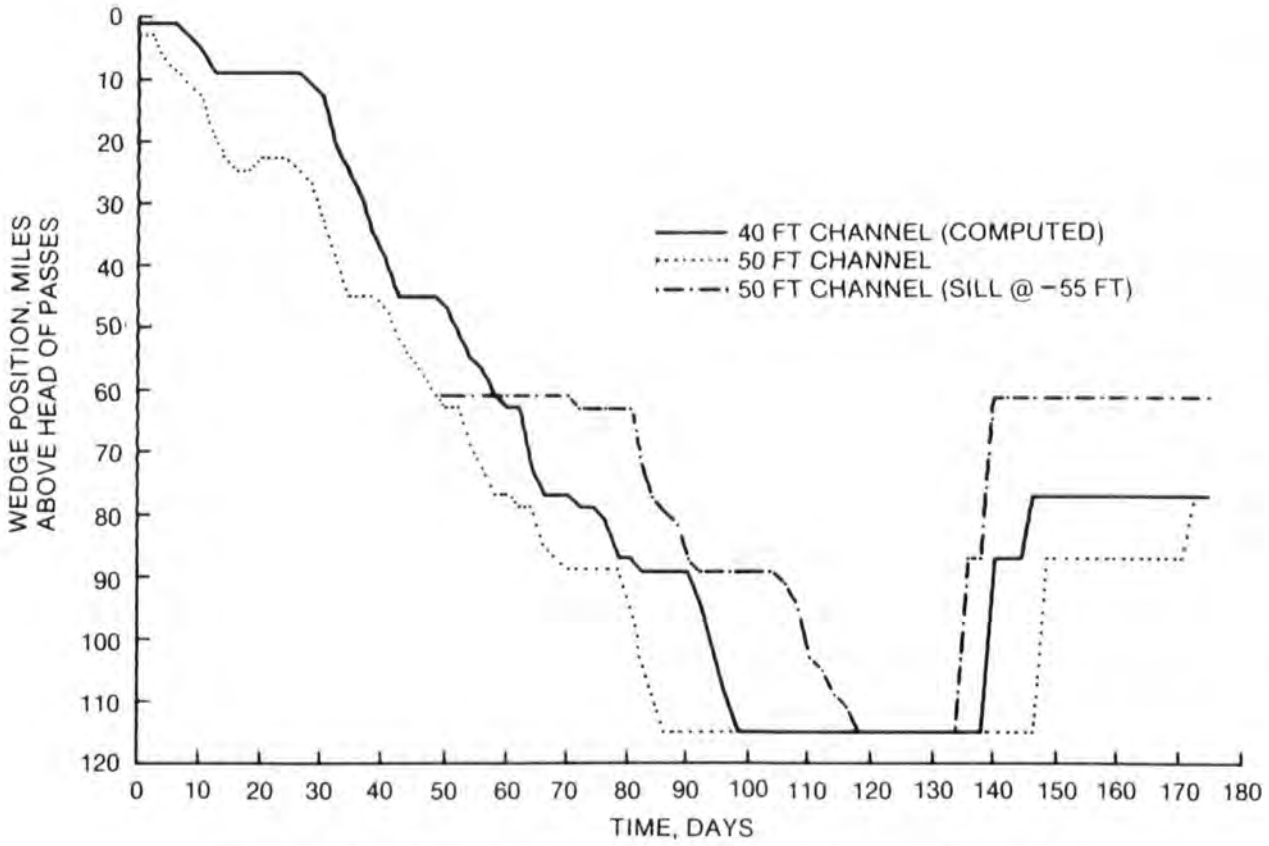

Figure 51. Effect of sill at mile 63.4 on salt wedge intrusion in the 50-ft channel for 1953-54 hydrograph

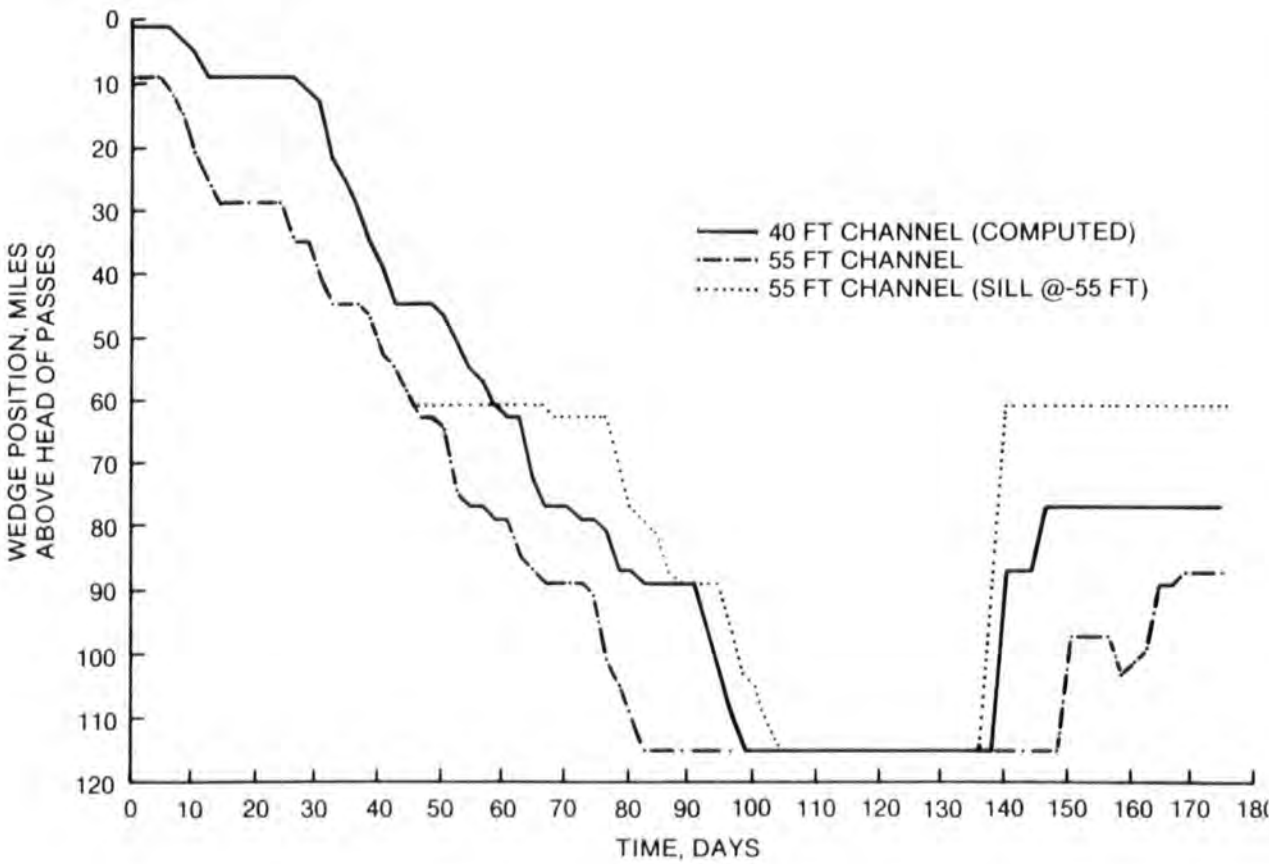

Figure 52. Effect of sill at mile 63.4 on salt wedge intrusion in the 55-ft channel for 1953-54 hydrograph

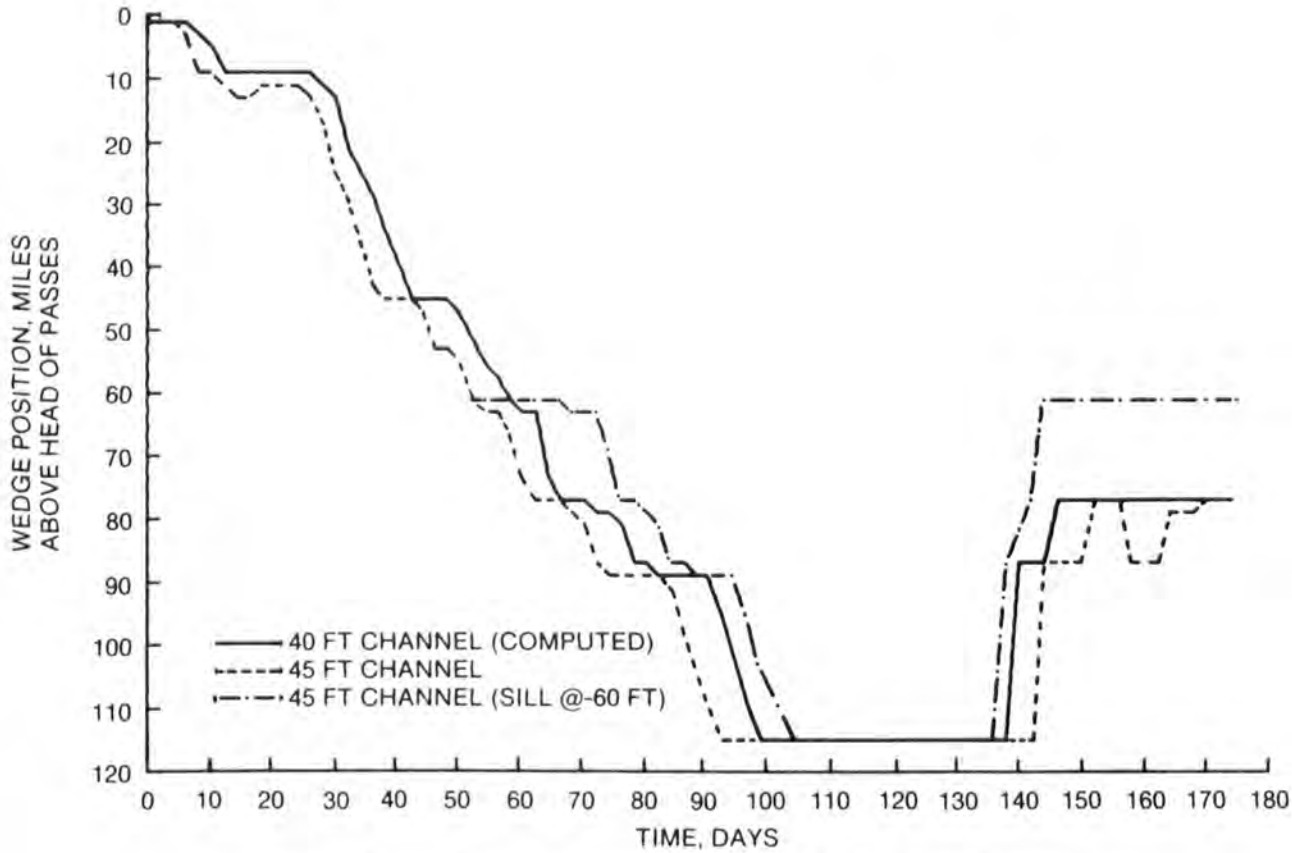

Figure 53. Effect of sill at mile 63.4 on salt wedge intrusion in the 45-ft channel for 1953-54 hydrograph

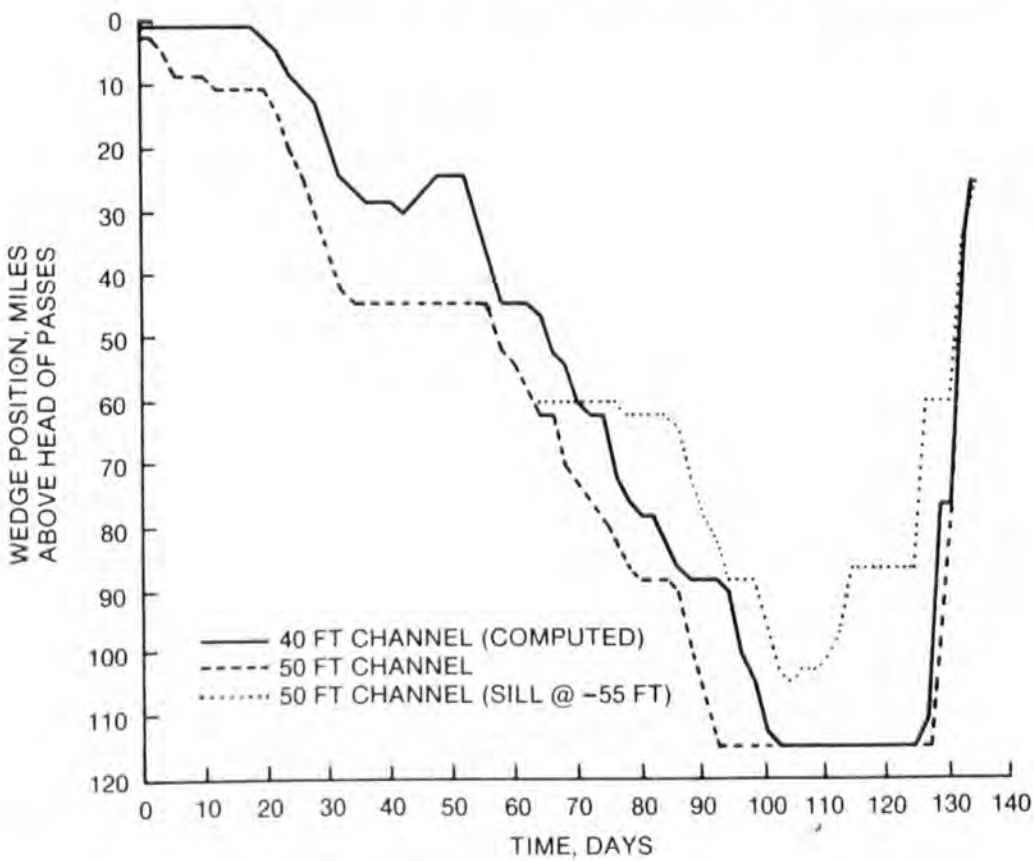

Figure 54. Effect of sill at mile 63.4 on salt wedge intrusion in the 50-ft channel for 1936 hydrograph

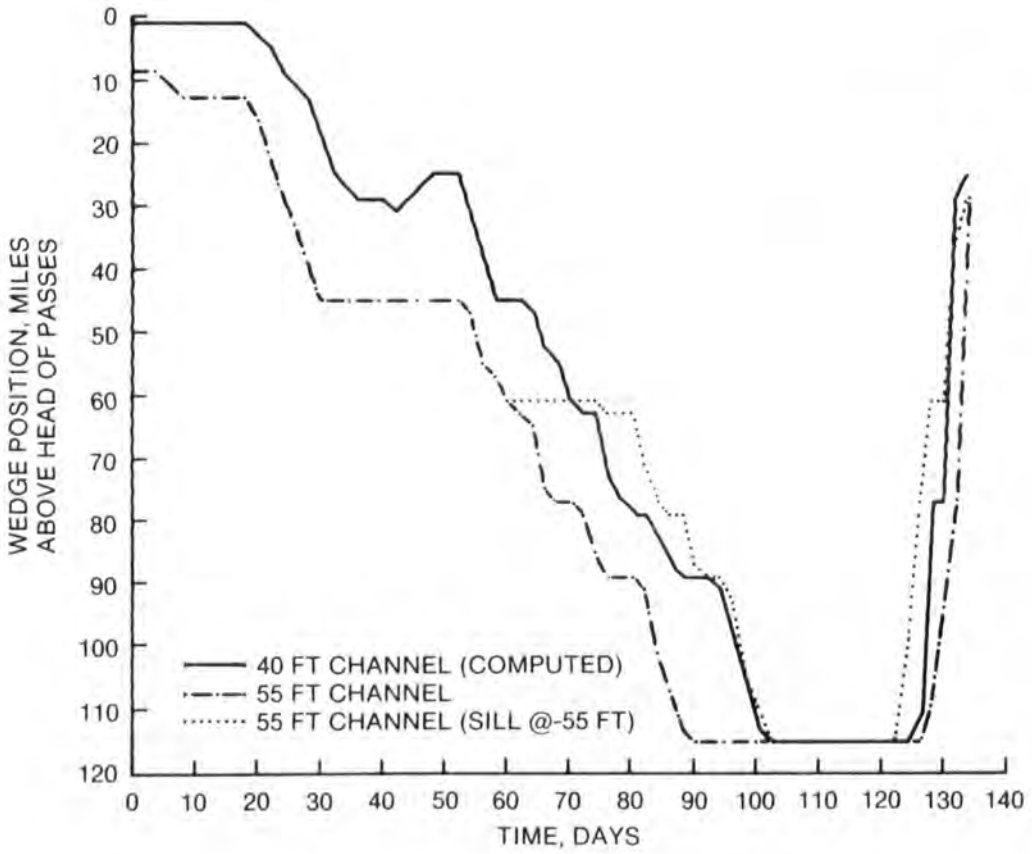

Figure 55. Effect of sill at mile 63.4 on salt wedge intrusion in the 55-ft channel for 1936 hydrograph

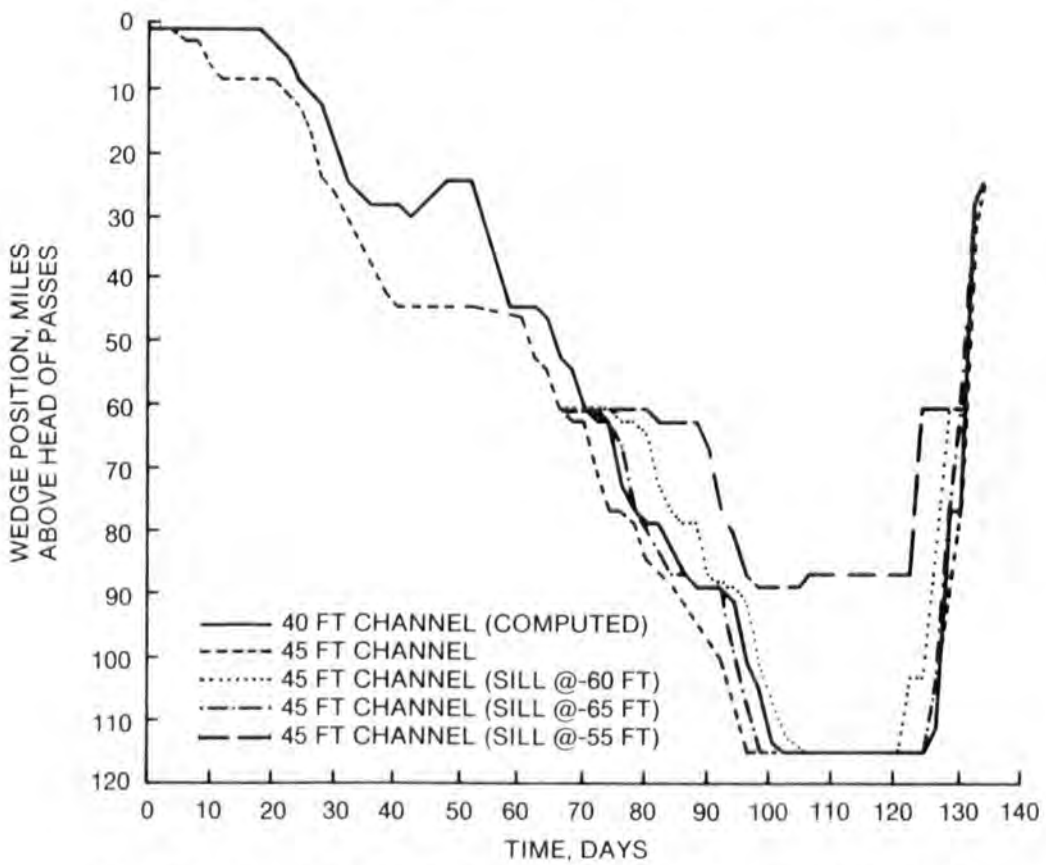

Figure 56. Effect of sill at mile 63.4 on salt wedge intrusion in the 45-ft channel for 1936 hydrograph

PART VIII: SUMMARY AND CONCLUSIONS

Summary

66. Since there is a concern that deepening Southwest Pass could significantly influence the salinity intrusion in the Lower Mississippi River, which in turn could have a serious impact on the supply of fresh water to New Orleans and other localities along the river, a dynamic analysis of the salinity intrusion phenomena using actual channel cross sections was authorized by LMN. To accomplish this, a numerical model called LAEM, which is a laterally averaged model that couples the computation of the flow and salinity fields through the influence of the salinity on the water density, has been employed.

67. After verifying the model using 1980-81 field data, several historical hydrographs furnished by LMN were run and results for 40-, 45-, 50-, and 55-ft channels have been presented. In addition, results from a series of steady-flow runs, obtained by using the model as previously verified without several of the river crossings below New Orleans, are presented and tend to support the intrusion curves developed several years ago by LMN.

68. The final application of the model was to test the impact on the intrusion of the salt wedge of increasing the height of the natural river crossing at about mile 63 by dredging the upstream channel and depositing the material on the crossing. An assessment of the stability of a sill built from natural river sediment was accomplished through an application of the HEC-6 computer program.

Conclusions

69. In general, it is concluded that the numerical model, LAEM, provides a very useful tool for assessing the impact of major changes in channel geometry on the intrusion of salinity. Verification of LAEM for the Lower Mississippi River produced a model whose computed results were in good agreement with the limited field data available and responded well to the various boundary data imposed. Particular conclusions from the salinity-intrusion computations reported herein follow:

a. Only the 1980-81 field data could be utilized to verify the

model since the shoaling of South Pass since 1973 has changed the manner in which the salt wedge is formed by saline water from the Gulf.

b. Computed wedge intrusion for earlier steady-flow tests in both the 40- and 55-ft channels was generally supportive of the intrusion curves developed by LMN.

c. Hydrograph tests for the 1980-81, 1968, 1955-56, 1953-54, 1952-53, 1947-48, 1938-39, and 1936 low-flow periods provide useful information on duration of wedge intrusion for these hydrographs and insight concerning the importance of hydrograph shape and channel crossings on the extent and duration of wedge intrusion.

d. Channel crossings, particularly the ones at miles 47, 77, 87, and 116, significantly limit the extent and duration of salinity intrusion in the Lower Mississippi River.

e. Results from runs with deepened channels revealed that deepening the channel will significantly increase the extent and duration of salinity intrusion.

f. The 1953-54 hydrograph resulted in the greatest intrusion and duration of the computed salt wedge, although the low flow of record on the Lower Mississippi River occurred during 1936 and historical data imply that more severe salinity conditions existed in 1936.

g. An interesting observation from the computations for the 1953-54 flows is that the wedge position for the 55-ft channel followed quite closely the field data collected during that time. Therefore, with channel conditions below the Head of Passes as they currently exist, the impact on salinity intrusion of deepening Southwest Pass to 55 ft may be to essentially return the wedge movement back to pre-1973 conditions before South Pass was allowed to shoal. Computations from an arrested wedge model tended to substantiate this conclusion.

h. Man-induced alterations to create greater heights at river crossings, i.e., to create a sill in the river, appear to be an effective means of limiting wedge intrusion during critically low-flow periods. For 1953-54 flow conditions and a 55-ft channel, a sill at mile 63 with a top elevation of -55 ft would result in salinity conditions at New Orleans similar to those that occur with the existing 40-ft channel.

70. Results from the sill stability tests with a -55-ft sill in a 55-ft channel indicate that the deposited material on the crossing will be eroded fairly quickly as the riverflow increases above 400,000 cfs, e.g., a constant riverflow of 700,000 cfs for 10 days will erode about 9 ft of the sill height. For riverflows below 400,000 cfs, the sill will be stable. These results imply that the sill will have to be reconstructed before each critical low-flow event.

REFERENCES

Balloffet, A., and Borah, D. K. 1985 (Feb). "Lower Mississippi Salinity Analysis," American Society of Civil Engineers, Hydraulics Division, Vol III, No. 2, pp 300-315.

Boyd, M. B., and Johnson, B. H. 1982. "Mississippi River Salinity Intrusion Study," Letter report to US Army Engineer District, New Orleans, New Orleans, La.

Copeland, R. W. 1983. "Sill Stability Results," Memorandum for Record, Hydraulic Analysis Division, Hydraulics Laboratory, US Army Engineer Waterways Experiment Station, Vicksburg, Miss.

Edinger, J. E., and Buchak, E. M. 1979. "A Hydrodynamic Two-Dimensional Reservoir Model: Development and Test Application to Sutton Reservoir, Elk River, West Virginia," prepared for US Army Engineer Division, Ohio River, Cincinnati, Ohio.

_____. 1981 (Nov). "Estuarine Laterally Averaged Numerical Dynamics; The Development and Testing of Estuarine Boundary Conditions in the LARM Code," Miscellaneous Paper EL-81-9, US Army Engineer Waterways Experiment Station, Vicksburg, Miss.

_____. 1983 (Jan). "Developments in LARM2: A Longitudinal-Vertical Time-Varying Hydrodynamic Reservoir Model," Technical Report E-83-1, US Army Engineer Waterways Experiment Station, Vicksburg, Miss.

Hydrologic Engineering Center (HEC). 1976. "Geometric Elements from Cross Sections Coordinates," Generalized Computer Program 723-G2-L745B, Davis, Calif.

_____. 1977. "Scour and Deposition in Rivers and Reservoirs," Generalized Computer Program 723-G2-L2470, Davis, Calif.

Keulegan, G. H. 1949. "The Determination of Salinities in Tests of Density Currents," NBS Report, Fourth Progress Report on Model Laws of Density Currents, Report to Chief of Engineers, US Army Corps of Engineers, Washington, DC.

Kolb, Charles. 1963. "Distribution of Soils Bordering the Mississippi River from Donaldsonville to Head of Passes," Technical Report 3-601, US Army Engineer Waterways Experiment Station, Vicksburg, Miss.

Leendertse, J. J. 1967. "Aspects of a Computational Model for Long-Period Water-Wave Propagation," RM-5294-PR, The Rand Corporation, Santa Monica, Calif.

Schijf, J. B., and Schonfeld, J. C. 1953. "Theoretical Considerations of the Motion of Salt and Fresh Water," Proceedings, Minnesota International Hydraulic Convention, IAHR.

Table 1

Variables Used in Computation of τ_i

River Mile	$\Delta\rho/\rho$	$\bar{u}$	h_1	δ	h_1/h_2	dh_2/dx
0.0	0.0235	1.248	29.41	-0.425	0.425	0.00019
4.0	0.0210	1.433	33.52	-0.446	0.504	0.00024
12.0	0.0180	1.126	43.90	-0.623	0.782	0.00020
16.0	0.0170	1.183	48.18	-0.676	0.930	0.00011
20.0	0.0165	1.151	50.57	-0.725	1.023	0.00013
24.0	0.0165	1.067	53.27	-0.771	1.140	0.00015
28.0	0.0165	1.126	56.42	-0.815	1.295	0.00019
32.0	0.0165	1.107	60.46	-0.877	1.529	0.00010
36.0	0.0160	1.093	62.61	-0.912	1.674	0.00010
40.0	0.0160	1.162	64.69	-0.945	1.840	0.00007
44.0	0.0160	1.082	66.25	-0.970	1.960	0.00008
48.0	0.0160	1.011	67.93	-0.992	2.118	0.00000
52.0	0.0075	0.980	67.90	-1.004	2.115	0.00014
56.0	0.0075	1.077	70.94	-1.034	2.440	0.00020
60.0	0.0068	0.900	75.25	-1.076	3.040	0.00000
64.0	0.0065	0.570	75.29	-1.072	3.040	--

Table 2

Increase of Duration of Wedge Intrusion (9 ppt), with a 45-ft Channel, Beyond River Locations, Days

Hydrograph	Port Sulfur, Mile 40	Algiers, Mile 96	New Orleans, Mile 103
1980-81	3	0	0
1968	18	0	0
1955-56	19	--	--
1953-54	5	11	11
1952-53	5	13	13
1947-48	6	0	0
1938-39	11	0	0
1936	15	5	5

Table 3

Increase of Duration of Wedge Intrusion (9 ppt), with a 50-ft Channel, Beyond River Locations, Days

Hydrograph	Port Sulfur, Mile 40	Algiers, Mile 96	New Orleans, Mile 103
1980-81	7	0	0
1968	29	0	0
1955-56	30	--	--
1953-54	8	19	20
1952-53	28	22	22
1947-48	29	0	0
1938-39	28	0	0
1936	26	9	9

Table 4

Increase of Duration of Wedge Intrusion (9 ppt), with a 55-ft Channel, Beyond River Locations, Days

Hydrograph	Port Sulfur, Mile 40	Algiers, Mile 96	New Orleans, Mile 103
1980-81	14	0	0
1968	46	0	0
1955-56	53	--	--
1953-54	10	40	27
1952-53	49	30	31
1947-48	35	14	12
1938-39	43	0	0
1936	30	14	14

Table 5

Decrease of Wedge Intrusion (9 ppt), in a 55-ft Channel, with a Sill at Elevation -55 at Mile 63, Beyond Particular Locations, Days

Hydrograph	Port Sulfur, Mile 40	Algiers, Mile 96	New Orleans, Mile 103
1953-54	0	30	31
1936	0	17	18